

NUMERICAL ANALYSIS OF MODULAR REGULARIZATION METHODS FOR THE BDF2 TIME DISCRETIZATION OF THE NAVIER-STOKES EQUATIONS

WILLIAM LAYTON*, NATHANIEL MAYST†, MONIKA NEDA‡, AND CATALIN TRENCHEA§

Abstract. We consider an uncoupled, modular regularization algorithm for approximation of the Navier-Stokes equations. The method is: Step 1: Advance the NSE one time step, Step 2: Regularize to obtain the approximation at the new time level. Previous analysis of this approach has been for simple time stepping methods in Step 1 and simple stabilizations in Step 2. In this report we extend the mathematical support for uncoupled, modular stabilization to (i) the more complex and better performing BDF2 time discretization in Step 1, and (ii) more general (linear or nonlinear) regularization operators in Step 2. We give a complete stability analysis, derive conditions on the Step 2 regularization operator for which the combination has good stabilization effects, characterize the numerical dissipation induced by Step 2, prove an asymptotic error estimate incorporating the numerical error of the method used in Step 1 and the regularizations consistency error in Step 2 and provide numerical tests.

1. Introduction. This report continues the numerical analysis of modular, uncoupled stabilization/regularization methods for (primarily under-resolved) flow problems, extending their analytical foundation from one step Crank-Nicolson (CN) method and linear filtering in [18] to the multi-step BDF2 time discretization and more general regularization operators herein. For Ω a polyhedral domain in \mathbb{R}^d , $d = 2, 3$, the fluid velocity $u(x, t)$ and pressure $p(x, t)$ satisfy:

$$\begin{aligned} u_t + u \cdot \nabla u - \nu \Delta u + \nabla p &= f(x, t) \text{ and } \nabla \cdot u = 0, \text{ in } \Omega \times (0, T], \\ u &= 0 \text{ on } \partial\Omega \text{ and } u(x, 0) = u^0(x) \text{ in } \Omega. \end{aligned}$$

The unavoidability of underresolved simulations has led to numerous regularizations and stabilizations in Computational Fluid Dynamics. The idea of “*evolve one time step then regularize*” fits well with the modular development of complex codes and with legacy codes. It was initiated by Boyd [8], Fischer and Mullen [19], [34], and used by Dunca [13]. A numerical analysis of the stability, dissipation and error behaviour in linear filter based stabilization of the Crank-Nicolson method with finite element discretization was performed in [18], including effects of deconvolution and relaxation. The case of backward Euler time discretization plus nonlinear filtering, and relaxation was considered in [31]. Mathew et al. [33] pointed that this stabilization induces a new implicit time relaxation term that acts to damp oscillations in marginally resolved scales. See also Section 5.3.3 in Garnier, Adams and Sagaut [20] and Visbal and Rizzetta [47]. The connection to time relaxation links the methods herein to work of Schochet and Tadmor [38], Roseneau [36], Adams, Kleiser, Leonard and Stolz [1], [2], [3], [40], [42], [41], [43], Dunca [13], [14], [15] and Layton, Neda, Manica, Rebholz, Ervin and Connors [30], [29], [17], [27], [12].

Let $X = (H_0^1(\Omega))^d$, $Q = L_0^2(\Omega)$; we let $X_h \subset X$, $Q_h \subset Q$ denote velocity, pressure finite element spaces satisfying the usual discrete inf-sup condition, see Section 2 for full details. Let $V_h \subset X_h$ denote the discretely divergence free subspace of X_h . We shall denote the regularization operator by the, possibly nonlinear, map $G_h : X \rightarrow V_h$; see Section 2 for examples of $G_h(\cdot)$.

ALGORITHM 1.1. [BDF2, Regularize, Relax for NSE]
Choose χ with $0 \leq \chi \leq 1$.

*Department of Mathematics, University of Pittsburgh, Pittsburgh, PA, 15260, USA. email: wjl@pitt.edu. Partially supported by the NSF under grant DMS-0810385.

†Department of Mathematics, University of Pittsburgh, Pittsburgh, PA, 15260, USA. email: nhm3@pitt.edu. Partially supported by the NSF under grant DMS-0810385.

‡Department of Mathematical Sciences, University of Nevada Las Vegas, USA. email: Monika.Neda@unlv.edu.

§Department of Mathematics, University of Pittsburgh, Pittsburgh, PA, 15260, USA. email: trenchea@pitt.edu. Partially supported by the Air Force under grant FA9550-09-1-0058.

Step 1 : Given u_h^n, u_h^{n-1} find $w_h^{n+1} \in X_h, p_h^{n+1} \in Q_h$ satisfying

$$\begin{aligned} & \left(\frac{3w_h^{n+1} - 4u_h^n + u_h^{n-1}}{2\Delta t}, v_h \right) + b^*(w_h^{n+1}, w_h^{n+1}, v_h) + \nu(\nabla w_h^{n+1}, \nabla v_h) \\ & - (p_h^{n+1}, \nabla \cdot v_h) = (f^{n+1}, v_h), \text{ for all } v_h \in X_h, \\ & (\nabla \cdot w_h^{n+1}, q_h) = 0, \text{ for all } q_h \in Q_h. \end{aligned} \quad (1.1)$$

Step 2 : Regularize w_h^{n+1} to give $G_h(w_h^{n+1})$, and relax

$$u_h^{n+1} = (1 - \chi)w_h^{n+1} + \chi G_h(w_h^{n+1}). \quad (1.2)$$

Step 1, without Step 2 of Algorithm 1.1 is the classical BDF2-FEM (finite element method) discretization of the Navier-Stokes equations analyzed in [4] (under a small data condition) and [16, 35, 48, 6]. The relaxation in (1.2) in Step 2 was introduced by Fischer and Mullen in [19], [34] to keep numerical diffusion from blowing up as $\Delta t \rightarrow 0$. If we denote the regularization error by

$$\epsilon(u) := \|u - G_h(u)\|$$

then the temporal consistency error of Algorithm 1.1 is $O(\Delta t^3 + \chi \epsilon(u))$ which forecasts a global error of $O(\Delta t^2 + \frac{\chi}{\Delta t} \epsilon(u) + \text{spatial FEM error})$. Attaining this forecasted error depends on the stability of Algorithm 1.1. The key requirements for stability of Algorithm 1.1 from Section 3 are: $0 \leq \chi \leq 1$ and

$$\begin{aligned} & (G_h(v), v) > 0 \text{ for all } v \neq 0, \\ & (v - G_h(v), G_h(v)) > 0 \text{ for all } v \neq 0. \end{aligned} \quad (1.3)$$

We give five examples of computationally attractive $G_h(\cdot)$ satisfying (1.3) in Section 2.1, and a complete numerical analysis of Algorithm 1.1 for general $G_h(\cdot)$ satisfying (1.3). Section 5 presents extensive tests of Algorithm 1.1 of underresolved flows.

2. Preliminaries. The $L^2(\Omega)$ norm and inner product will be denoted by $\|\cdot\|$ and (\cdot, \cdot) . The $L^p(\Omega)$ and the Sobolev $W_p^k(\Omega)$ norms are denoted by $\|\cdot\|_{L^p}$ and $\|\cdot\|_{W_p^k}$, respectively and the seminorm by $|\cdot|_{W_p^k}$. H^k is used to represent the Sobolev space $W_2^k(\Omega)$, and $\|\cdot\|_k$ denotes the norm in H^k . The space H^{-k} denotes the dual space of H_0^k . For functions $v(x, t)$ defined on the entire time interval $(0, T)$, we define $(1 \leq m < \infty)$

$$\|v\|_{\infty, k} := \text{EssSup}_{[0, T]} \|v(t, \cdot)\|_k, \text{ and } \|v\|_{m, k} := \left(\int_0^T \|v(t, \cdot)\|_k^m dt \right)^{1/m}.$$

We shall assume that the solution to the NSE that is approximated is a strong solution and in particular satisfies

$$u \in L^2(0, T; X) \cap L^\infty(0, T; L^2(\Omega)) \cap L^4(0, T; X), \quad (2.1)$$

$$p \in L^2(0, T; Q), \quad u_t \in L^2(0, T; X^*), \quad (2.2)$$

and

$$(u_t, v) + (u \cdot \nabla u, v) - (p, \nabla \cdot v) + \nu(\nabla u, \nabla v) = (f, v) \quad \forall v \in X, \quad (2.3)$$

$$(\nabla \cdot u, q) = 0 \quad \forall q \in Q. \quad (2.4)$$

We take

$$X := (H_0^1(\Omega))^d, \quad Q := L_0^2(\Omega).$$

We use as the norm on X the H^1 seminorm which, because of the boundary condition, is a norm, i.e. for $v \in X$, $\|v\|_X := \|\nabla v\|_{L^2}$. The space of divergence free functions is given by

$$V := \{v \in X : (\nabla \cdot v, q) = 0 \quad \forall q \in Q\}.$$

We shall denote conforming velocity, pressure finite element spaces based on an edge to edge triangulations of Ω (with maximum triangle diameter h) by

$$X_h \subset X, \quad Q_h \subset Q.$$

We shall assume that (X_h, Q_h) satisfy the usual inf-sup condition necessary for the stability of the pressure, e.g. [21, 22] and that the usual approximation properties of piecewise polynomials of degree k , $k-1$ hold for (X_h, Q_h) . The discretely divergence free subspace of X_h is

$$V_h = \{v_h \in X_h : (\nabla \cdot v_h, q_h) = 0 \quad \forall q_h \in Q_h\}.$$

Taylor-Hood elements (see e.g. [9, 21]) are one common example of such a choice with $k=2$ for (X_h, Q_h) , and are also the elements we use in our numerical experiments. Define the usual explicitly skew symmetrized trilinear form

$$b^*(u, v, w) := \frac{1}{2}(u \cdot \nabla v, w) - \frac{1}{2}(u \cdot \nabla w, v).$$

To set notation, let

$$t^n = n\Delta t, \quad n = 0, 1, 2, \dots, N_T, \quad T := N_T\Delta t, \quad \text{and} \quad d_t f^n := \frac{f(t^n) - f(t^{n-1})}{\Delta t}.$$

Introduce the following discrete norms

$$\|v\|_{\infty, k} := \max_{0 \leq n \leq N_T} \|v^n\|_k, \quad \|v\|_{m, k} := \left(\Delta t \sum_{n=0}^{N_T} \|v^n\|_k^m \right)^{1/m}.$$

PROPOSITION 2.1. *Under assumptions (1.3), the regularization map G_h satisfies additionally: for all $v \in X$*

$$0 < (v - G_h(v), v), \quad v \neq 0, \tag{2.5}$$

$$(G_h(v), v) \leq \|v\|^2, \tag{2.6}$$

$$(v - G_h(v), v) \leq \|v\|^2. \tag{2.7}$$

Proof. For all $v \in X$ we have that

$$(v - G_h(v), v) = \|v - G_h(v)\|^2 + (v - G_h(v), G_h(v)) \geq (v - G_h(v), G_h(v))$$

and (2.5) follows immediately from (1.3). To prove the second claim, note that

$$(G_h(v), v) = \|v\|^2 - (v - G_h(v), v)$$

and use (2.5). Finally, by (1.3) we obtain

$$(v - G_h(v), v) = \|v\|^2 - (G_h(v), v) \leq \|v\|^2.$$

□

The work of computing the action of a general, nonlinear regularization operator $G(\phi)$ can be considerable.

ASSUMPTION 2.2. *We shall thus restrict $G_h(\cdot)$ to be semilinear, i.e.,*

$$G_h(\phi) = \mathcal{G}_h(\phi)\phi$$

where $\forall w \in X, \mathcal{G}_h(w) \in \mathcal{L}(V_h, V_h)$ is a linear and continuous operator.

This restriction means, given $\widehat{\phi}$, computing the action $\phi \rightarrow \mathcal{G}_h(\widehat{\phi})\phi$ (even for $\widehat{\phi} = \phi$) requires linear work. This restriction includes the case of $\mathcal{G}_h(\cdot)$ being fixed linear operator (e.g. a linear filter) and also plays a key role in the error analysis.

In the remainder we impose, instead of the positivity condition (1.3), the following related uniform positivity assumption.

ASSUMPTION 2.3. *For any $w \in X$, the linear operator $\mathcal{G}_h(w) \in \mathcal{L}(V_h, V_h)$ satisfies*

$$(\mathcal{G}_h(w)\phi, \phi) > 0 \text{ for all } \phi \neq 0, \quad (2.8)$$

$$(\phi - \mathcal{G}_h(w)\phi, \mathcal{G}_h(w)\phi) > 0 \text{ for all } \phi \neq 0. \quad (2.9)$$

Clearly Assumption 2.3 implies (1.3), and for linear regularizations they are equivalent. Following the proof of Proposition 2.1, we note that, under Assumption 2.3, $\mathcal{G}_h(w)$ is non-expansive and

$$0 < ((I - \mathcal{G}_h(w))v, v) \leq \|v\|^2 \text{ for all } v \neq 0. \quad (2.10)$$

2.1. Examples of Regularization Operators. We collect several regularizations studied previously. Here $\delta > 0$ denotes a regularization length scale and $\phi \in L^2(\Omega)$.

1. Discrete differential filter. The discrete differential filter $G_h : L^2(\Omega) \rightarrow X_h$, is given as $G_h(\phi) := \overline{\phi}_h$, where $\overline{\phi}_h \in X_h$ is the unique solution of

$$\delta^2(\nabla \overline{\phi}_h, \nabla v_h) + (\overline{\phi}_h, v_h) = (\phi, v_h) \quad \forall v_h \in X_h. \quad (2.11)$$

2. Discrete Stokes differential filter. The discrete Stokes differential filter is often necessary to preserve discrete incompressibility. $G_h : X^* \rightarrow X_h$, and $\overline{\phi}_h = G_h(\phi)$ where $(\overline{\phi}_h, \rho) \in X_h \times Q_h$ is the unique solution of

$$\begin{aligned} \delta^2(\nabla \overline{\phi}_h, \nabla v_h) + (\overline{\phi}_h, v_h) - (\rho, \nabla \cdot v_h) &= (\phi, v_h) \quad \forall v_h \in X_h, \\ (\nabla \cdot \overline{\phi}_h, q) &= 0 \quad \forall q \in Q_h. \end{aligned} \quad (2.12)$$

The choices (2.11) and (2.12) of G_h satisfy (1.3), with regularization error (e.g. Lemma 2.1 in [18])

$$\epsilon(\phi) + \delta^2 \|\nabla(\phi - G_h(\phi))\|^2 \leq C \inf_{v_h \in V_h} \{ \delta^2 \|\nabla(\phi - v_h)\|^2 + \|\phi - v_h\|^2 \} + C\delta^4 \|\Delta\phi\|^2.$$

3. Nonlinear filters. Select a smooth function $a : X \rightarrow \mathbb{R}$, $a = a(\phi, \nabla\phi, \dots)$ (denoted by $a(\phi)$) with the properties

$$0 < a_{\min} \leq a(\phi) \leq 1 \quad \text{for any } \phi \in V,$$

see [31] for examples of such $a(\cdot)$. Define $G_h(\phi) := \overline{\phi}_h$ as the unique solution of: find $(\overline{\phi}_h, \lambda_h) \in X_h \times Q_h$ satisfying

$$(\delta^2 a(\phi) \nabla \overline{\phi}_h, \nabla v_h) + (\overline{\phi}_h, v_h) - (\lambda_h, \nabla \cdot v_h) = (\phi, v_h) \quad \forall v_h \in X_h, \quad (2.13)$$

$$(\nabla \cdot \overline{\phi}_h, q) = 0 \quad \forall q \in Q_h. \quad (2.14)$$

Note that $\bar{\phi}_h := G_h(\phi) = \mathcal{G}_h(\phi)\phi$, where the linear and continuous operator $\mathcal{G}_h(w)\phi := \tilde{\phi}$ is the unique solution $(\tilde{\phi}_h, \lambda_h) \in X_h \times Q_h$ of

$$(\delta^2 a(w) \nabla \tilde{\phi}^h, \nabla v_h) + (\tilde{\phi}^h, v_h) - (\lambda_h, \nabla \cdot v_h) = (\phi, v_h) \quad \forall v_h \in X_h, \quad (2.15)$$

$$(\nabla \cdot \tilde{\phi}^h, q) = 0 \quad \forall q \in Q_h. \quad (2.16)$$

LEMMA 2.4. *Let $G_h(\cdot)$ be the nonlinear filter (2.13)-(2.14). Assumption 2.3 holds. Thus (1.3) holds as well: for all $\phi \in V_h$ we have*

$$\begin{aligned} (G_h(\phi), \phi) &> 0, & \text{and} & \quad (\mathcal{G}_h(w)\phi, \phi) > 0 \quad \text{for all } w, \phi \neq 0 \\ (\phi - G_h(\phi), G_h(\phi)) &> 0, & & \quad (\phi - \mathcal{G}_h(w)\phi, \mathcal{G}_h(w)\phi) > 0 \quad \text{for all } w, \phi \neq 0. \end{aligned}$$

Proof. It is sufficient to prove that any $w \in X, \mathcal{G}_h(w)$ satisfies (2.8), (2.9). For $v_h \in V_h$ (2.15)-(2.16) are equivalent to:

$$(\delta^2 a(w) \nabla \tilde{\phi}_h, \nabla v_h) + (\tilde{\phi}_h, v_h) = (\phi, v_h) \quad \forall v_h \in V_h.$$

To prove the first assertion, set $v_h = \tilde{\phi}_h$. We then have

$$(\mathcal{G}_h(w)\phi, \phi) = (\phi, \tilde{\phi}_h) = \int_{\Omega} \delta^2 a(w) |\nabla \tilde{\phi}_h|^2 + |\tilde{\phi}_h|^2.$$

For the second claim, note that

$$(\phi - \tilde{\phi}_h, \tilde{\phi}_h) = \int_{\Omega} \delta^2 a(w) |\nabla \tilde{\phi}_h|^2 dx \geq \delta^2 a_{\min} \|\nabla \tilde{\phi}_h\|^2.$$

This is positive for $\phi \neq 0$. Indeed, if $\|\nabla \tilde{\phi}_h\|^2 = 0$, then $\tilde{\phi}_h \equiv 0$ (due to the zero boundary conditions) and then $(\phi, v_h) = 0 \quad \forall v_h \in V_h$. \square

It has been shown in [31] that the nonlinear filter (2.13)-(2.14) has the following regularization error.

THEOREM 2.5. *Let X_h, Q_h satisfy the inf-sup condition and $\phi \in V$. Then the discrete nonlinear filter $G_h(\phi)$ given by (2.13)-(2.14) satisfies*

$$\begin{aligned} &\epsilon(\phi) + \int_{\Omega} \delta^2 a(\phi) |\nabla(\phi - G_h(\phi))|^2 dx \\ &\leq C \inf_{\hat{\phi} \in V_h} \left\{ \int_{\Omega} \delta^2 a(\phi) |\nabla(\phi - \hat{\phi})|^2 dx + \|\phi - \hat{\phi}\|^2 \right\} + C \delta_{\max}^4 \|\nabla \cdot (a(\phi) \nabla \phi)\|^2. \end{aligned}$$

For the frozen nonlinearity discrete nonlinear filter (2.15)-(2.16): for any given $w_h \in V_h$, we have that for all $\phi \in V$

$$\begin{aligned} &\int_{\Omega} \delta^2 a(w_h) |\nabla(\phi - \mathcal{G}_h(w_h)\phi)|^2 dx + \|\phi - \mathcal{G}_h(w_h)\phi\|^2 \\ &\leq C \inf_{\hat{\phi} \in V_h} \left\{ \int_{\Omega} \delta^2 a(w_h) |\nabla(\phi - \hat{\phi})|^2 dx + \|\phi - \hat{\phi}\|^2 \right\} + C \delta^2 \min\{\|\nabla \phi\|^2, \delta^2 \|\nabla \cdot (a(w_h) \nabla \phi)\|^2\}. \end{aligned} \quad (2.17)$$

4. Modular VMS methods. Let $X_H \subset X_h, Q_H \subset Q_h$ denote subspaces of the velocity-pressure FEM spaces associated typically with either lower degree polynomials on the same mesh or the same finite

element spaces on a coarser mesh. Define $P_H : \nabla X_h \rightarrow \nabla X_H$ to be the L^2 projection operator. Let ν_T be a bounded, positive, elementwise constant, eddy viscosity parametrization and $\delta > 0$ the filter lengthscale. The modular VMS regularization operator introduced in [32] is the linear operator $G_h(\phi) = \bar{\phi} \in V_h$, the solution of

$$(\nu_T[I - P_H]\nabla\bar{\phi}, [I - P_H]\nabla v_h) + (\bar{\phi}, v_h) = (\phi, v_h) \text{ for all } v_h \in V_h. \quad (2.18)$$

LEMMA 2.6. $G_h(\cdot)$, defined by (2.18), satisfies (1.3): for all $\phi \in X_h$

$$(G_h(\phi), \phi) > 0 \quad \text{and} \quad (\phi - G_h(\phi), G_h(\phi)) \geq 0.$$

Proof. The proof is similar to the Lemma 2.4. For the first claim set $v_h = \bar{\phi}$ in (2.18). For the second claim set $v_h = \bar{\phi}$ again. We have

$$(\phi - \bar{\phi}, \bar{\phi}) = \int_{\Omega} \nu_T |[I - P_H]\nabla\bar{\phi}|^2 dx \geq 0. \quad \square$$

Note that $\nabla\bar{\phi}$ is the L^2 projection into ∇X_H , thus provided $\phi \in H^2(\Omega)$

$$\epsilon(\phi) = \|\phi - G_h(\phi)\| \leq CH\|\nabla\phi\|.$$

5. Approximate Deconvolution. One rich source of high accuracy regularization operators is approximate deconvolution of a filter F_h . (such as the filters in examples 1 and 2). The van Cittert deconvolution operator is defined using powers of $(I - F_h)$ as follows.

DEFINITION 2.7 (Discrete van Cittert deconvolution). *Let $\bar{\phi} = F_h(\phi)$ be a linear filter satisfying Assumption 2.3. Then the N^{th} discrete van Cittert operator is:*

$$D_h^N \phi := \sum_{n=0}^N (I - F_h)^n \phi.$$

We then define $G_h(\phi) = D_h^N \bar{\phi}$. In [18] the conditions (1.3) were proven for F_h being the discrete Stokes filter.

LEMMA 2.8. *We have $D_h^N : V_h \rightarrow V_h$ and for all $\phi \in V_h$*

$$(D_h^N(\bar{\phi}), \phi) > 0 \text{ and } (\phi - D_h^N(\bar{\phi}), D_h^N(\bar{\phi})) > 0 \text{ if } \phi \neq 0, \\ \|D_h^N(\bar{\phi})\| \leq \|\phi\| \text{ and } \|\phi - D_h^N(\bar{\phi})\| \leq \|\phi\|.$$

Proof. Using the symmetry and linearity of F_h , and Assumption 2.3 for F_h , we have

$$\begin{aligned} (D_h^N(\bar{\phi}), \phi) &= \sum_{i=0}^{\lfloor \frac{N}{2} \rfloor} \left(\left[(I - F_h)^{2i} + (I - F_h)^{2i+1} \right] (\bar{\phi}), \phi \right) + (1 - 2\{\frac{N}{2}\}) \left((I - F_h)^N(\bar{\phi}), \phi \right) \\ &= \sum_{i=0}^{\lfloor \frac{N}{2} \rfloor} \left(2 \left((I - F_h)(I - F_h)^i \phi, F_h(I - F_h)^i \phi \right) + \|F_h(I - F_h)^i \phi\|^2 \right) \\ &\quad + (1 - 2\{\frac{N}{2}\}) \left(F_h(I - F_h)^{\lfloor \frac{N}{2} \rfloor} \phi, (I - F_h)^{\lfloor \frac{N}{2} \rfloor} \phi \right) > 0. \end{aligned}$$

To prove the second estimate, we note first that $\phi - D_h^N(\bar{\phi}) = (I - F_h)^{N+1} \phi$, and therefore

$$\begin{aligned} (\phi - D_h^N(\bar{\phi}), D_h^N(\bar{\phi})) &= \sum_{i=0}^{\lfloor \frac{N}{2} \rfloor} \left(\left[(I - F_h)^{2i+N+1} + (I - F_h)^{2i+N+2} \right] (\bar{\phi}), \phi \right) + (1 - 2\{\frac{N}{2}\}) \left((I - F_h)^{2N+1}(\bar{\phi}), \phi \right) > 0. \end{aligned}$$

The last two estimates follow as in the proof of Proposition 2.1. (See also [18] and Stanculescu [39].)
 \square We also use the following from [29].

LEMMA 2.9. *For smooth ϕ the discrete N^{th} order discrete approximate deconvolution regularization operator satisfies for $0 \leq s \leq N$*

$$\epsilon(\phi) = \|\phi - D_h^N(\bar{\phi})\| \leq C_1 \delta^{2s+2} \|\bar{\phi}\|_{H^{2s+2}} + C_2 (\delta h^k + h^{k+1}) \sum_{n=1}^{N+1} |F_h^n(\phi)|_{k+1}. \quad (2.19)$$

The dependence of the $|F_h^n(\phi)|_{k+1}$ terms in (2.19) upon the *filter radius* δ , for a general smooth function ϕ , is not fully understood. In the case of ϕ periodic the $|F_h^n(\phi)|_{k+1}$ are independent of δ . Also, for ϕ satisfying homogeneous Dirichlet boundary conditions, with the additional property that $\Delta^j \phi = 0$ on $\partial\Omega$ for $0 \leq j \leq \lfloor \frac{k+1}{2} \rfloor - 1$, the $|F_h^n(\phi)|_{k+1}$ are also independent of δ , see [29], [28].

The Taylor-Hood elements are a common choice for (X_h, Q_h) and correspond to $k = 2$ in (2.19). For these we have the following corollary.

COROLLARY 2.10. *Suppose $\phi \in H_0^1(\Omega) \cap H^4(\Omega)$. Suppose the order of deconvolution is $N = 1$ and (X_h, Q_h) are chosen to be the Taylor-Hood elements. We have*

$$\epsilon(\phi) = \|\phi - D_h^N(\bar{\phi})\| \leq C_1 \delta^3 \|\phi\|_3 + C_2 (\delta h^2 + h^3) \|\phi\|_3. \quad (2.20)$$

Proof. This follows from Lemma 2.9 by taking $s = 1/2$, $k = 2$, $N = 1$ and thus $\lfloor \frac{k+1}{2} \rfloor - 1 = 0$. We have then $\|\bar{\phi}\|_3 \leq C \|\phi\|_3$ with uniform constant. \square

Motivated by the above result for Hood-Taylor elements, in the (even) higher order case we will make the following assumption in the convergence analysis.

Assumption DG1: *Let $D_h^N(\cdot)$ be the van Cittert regularization operator. For some $\alpha, 0 < \alpha \leq N$*

$$\epsilon(\phi) = \|\phi - D_h^N(\bar{\phi})\| \leq C_1 \delta^{2\alpha+2} \|\phi\|_{H^{2\alpha+2}} + C_2 (\delta h^k + h^{k+1}) \|\phi\|_{k+1}. \quad (2.21)$$

3. Stability of Algorithm 1.1. We prove an energy equality, unconditional stability and give the precise formula for the numerical dissipation induced by the regularization operator in Step 2 of Algorithm 1.1. We begin the stability analysis with an algebraic identity.

LEMMA 3.1. [18, 31] *Assume $\chi \in [0, 1]$ and let $u_h = (1 - \chi)w_h + \chi G_h(w_h)$. Then*

$$\begin{aligned} \|w_h\|^2 - \|u_h\|^2 &= \chi(2 - \chi)(w_h - G_h(w_h), w_h) + \chi^2(w_h - G_h(w_h), G_h(w_h)), \\ \|w_h\|^2 - \|u_h\|^2 &= -\|u_h - w_h\|^2 + 2\chi(w_h - G_h(w_h), w_h). \end{aligned} \quad (3.1)$$

Proof. The proof is the same as in the case where G_h is a linear operator in [18, 31]. \square

DEFINITION 3.2. *Let $\|\cdot\|_{\chi,h}$ denote the following functional (non-negative by Assumptions (1.3) and Proposition 2.1)*

$$\|v\|_{\chi,h}^2 = ((1 - \chi)v + \chi G_h(v), \chi(v - G_h(v))), \text{ for all } v \in X_h.$$

While not a norm when $G_h(\cdot)$ is a nonlinear regularization, for G_h an SPD linear operator, $\|\cdot\|_{\chi,h}$ is a weighted norm on X_h .

PROPOSITION 3.3. [Stability] *Suppose that Assumption 2.3 holds. Then the Algorithm 1.1 satisfies the energy equality*

$$\begin{aligned}
& \frac{1}{4} \|u_h^{n+1}\|^2 + \frac{1}{4} \|2u_h^{n+1} - u_h^n\|^2 + \Delta t \sum_{j=1}^n \frac{\Delta t^3}{4} \left\| \frac{u_h^{j+1} - 2u_h^j + u_h^{j-1}}{\Delta t^2} \right\|^2 \\
& + \Delta t \sum_{j=1}^n \frac{3\chi}{2\Delta t} (w_h^{n+1} - G_h(w_h^{n+1}), w_h^{n+1}) + \frac{1}{4} \|w_h^{n+1}\|_{\chi,h}^2 + \frac{1}{4} \|2w_h^{n+1} - w_h^n\|_{\chi,h}^2 \\
& + \Delta t \sum_{j=1}^n \frac{\Delta t^3}{4} \| \frac{w_h^{j+1} - 2w_h^j + w_h^{j-1}}{\Delta t^2} \|_{\chi,h}^2 + \nu \Delta t \sum_{j=1}^n \|\nabla w_h^{n+1}\|^2 \\
& = \frac{1}{4} \|u_h^1\|^2 + \frac{1}{4} \|2u_h^1 - u_h^0\|^2 + \Delta t \sum_{j=1}^n (f^{j+1}, w_h^{j+1}),
\end{aligned}$$

and the stability bound

$$\begin{aligned}
& \frac{1}{4} \|u_h^{n+1}\|^2 + \frac{1}{4} \|2u_h^{n+1} - u_h^n\|^2 + \Delta t \sum_{j=1}^n \frac{\Delta t^3}{4} \left\| \frac{u_h^{j+1} - 2u_h^j + u_h^{j-1}}{\Delta t^2} \right\|^2 \\
& + \Delta t \sum_{j=1}^n \frac{3\chi}{2\Delta t} (w_h^{j+1} - G_h(w_h^{j+1}), w_h^{j+1}) + \frac{1}{4} \|w_h^{n+1}\|_{\chi,h}^2 + \frac{1}{4} \|2w_h^{n+1} - w_h^n\|_{\chi,h}^2 \\
& + \Delta t \sum_{j=1}^n \frac{\Delta t^3}{4} \| \frac{w_h^{j+1} - 2w_h^j + w_h^{j-1}}{\Delta t^2} \|_{\chi,h}^2 + \frac{\nu}{2} \Delta t \sum_{j=1}^n \|\nabla w_h^{n+1}\|^2 \\
& \leq \frac{1}{4} \|u_h^1\|^2 + \frac{1}{4} \|2u_h^1 - u_h^0\|^2 + \frac{\Delta t}{2\nu} \sum_{j=1}^n \|f^{j+1}\|_*^2.
\end{aligned}$$

Proof. In Step 1 in Algorithm 1.1 set $v_h = w_h^{n+1}$. Using the identity

$$\frac{1}{4} [a^2 + (2a - b)^2] - \frac{1}{4} [b^2 + (2b - c)^2] + \frac{1}{4} (a - 2b + c)^2 = \frac{1}{2} (3a - 4b + c)a, \quad (3.2)$$

this gives

$$\begin{aligned}
& \frac{1}{4\Delta t} (\|u_h^{n+1}\|^2 + \|2u_h^{n+1} - u_h^n\|^2) - \frac{1}{4\Delta t} (\|u_h^n\|^2 + \|2u_h^n - u_h^{n-1}\|^2) \\
& + \frac{1}{4\Delta t} \|u_h^{n+1} - 2u_h^n + u_h^{n-1}\|^2 + \frac{3}{2\Delta t} (\chi(w_h^{n+1} - G_h(w_h^{n+1})), w_h^{n+1}) \\
& + \frac{1}{4\Delta t} (\|w_h^{n+1}\|_{\chi,h}^2 + \|2w_h^{n+1} - w_h^n\|_{\chi,h}^2) - \frac{1}{4\Delta t} (\|w_h^n\|_{\chi,h}^2 + \|2w_h^n - w_h^{n-1}\|_{\chi,h}^2) \\
& + \frac{1}{4\Delta t} \|w_h^{n+1} - 2w_h^n + w_h^{n-1}\|_{\chi,h}^2 + \nu \|\nabla w_h^{n+1}\|^2 \\
& = (f^{n+1}, w_h^{n+1}).
\end{aligned}$$

Multiplying by Δt and summing, with the assumption $w_h^0 = w_h^1 = 0$, we obtain the energy equality

$$\begin{aligned}
& \frac{1}{4} \|u_h^{n+1}\|^2 + \frac{1}{4} \|2u_h^{n+1} - u_h^n\|^2 + \Delta t \sum_{j=1}^n \frac{1}{4\Delta t} \|w_h^{j+1} - 2w_h^j + w_h^{j-1}\|^2 \\
& + \Delta t \sum_{j=1}^n \frac{3\chi}{2\Delta t} (w_h^{n+1} - G_h(w_h^{n+1}), w_h^{n+1}) + \frac{1}{4} \|w_h^{n+1}\|_{\chi,h}^2 + \frac{1}{4} \|2w_h^{n+1} - w_h^n\|_{\chi,h}^2 \\
& + \Delta t \sum_{j=1}^n \frac{1}{4\Delta t} \|w_h^{j+1} - 2w_h^j + w_h^{j-1}\|_{\chi,h}^2 + \nu \Delta t \sum_{j=1}^n \|\nabla w_h^{n+1}\|^2 \\
& = \frac{1}{4} \|u_h^1\|^2 + \frac{1}{4} \|2u_h^1 - u_h^0\|^2 + \Delta t \sum_{j=1}^n (f^{j+1}, w_h^{j+1}).
\end{aligned}$$

Using the Cauchy-Schwarz-Young inequality on the right hand side and subsuming one term into the LHS proves global stability. \square

Let denote

$$D_+ D_- v^{n-1} = \frac{v^n - 2v^{n-1} + v^{n-2}}{\Delta t^2}.$$

The dissipation in Algorithm 1.1 is composed of the following terms in the energy equality:

$$\text{Viscous / Molecular Dissipation} := \nu \|\nabla w_h^{n+1}\|^2,$$

$$\text{Numerical Dissipation from Step 1} := \frac{\Delta t^3}{4} \|D_+ D_- u_h^n\|^2$$

$$\text{Numerical Dissipation from Step 2} := \frac{3\chi}{2\Delta t} (w_h^{n+1} - G_h(w_h^{n+1}), w_h^{n+1}) + \frac{\Delta t^3}{4} \|D_+ D_- w_h^n\|^2.$$

4. Error Analysis of the Algorithm 1.1.

In this section we present a detailed error analysis. We first establish computability of the procedure.

LEMMA 4.1. *Assume $\chi \in [0, 1]$ and Assumptions 2.2, 2.3 hold. For Algorithm 1.1, w_h^n, u_h^n exist at each time step.*

Proof. The existence of a solution w_h^n to (1.1) follows from the Leray-Schauder Principle [49]. Specifically, with $A : V_h \rightarrow V_h$, defined by $y = A(w)$

$$(y, v) := -\frac{2\Delta t}{3} b^*(w, w, v) - \frac{2\Delta t}{3} \nu (\nabla w, \nabla v) + \frac{1}{3} (4u_h^{n-1} - u_h^{n-2}, v) + \frac{2\Delta t}{3} (f^n, v),$$

the operator A is compact and any solution of $w = sA(w)$, for $0 \leq s < 1$, satisfies the bound $\|w\| \leq \gamma$, where γ is independent of s .

The existence and uniqueness of $\overline{w_h^n}$ follows directly from the assumption on the well-posedness of the regularization operator. The existence and uniqueness of u_h^n follows from that for w_h^n and $\overline{w_h^n}$ and the definition of G_h . \square

In order to establish the optimal asymptotic error estimates for the approximation we need to assume that the true solution is more regular than that given by (2.1),(2.2).

$$u \in L^\infty(0, T; W_4^{k+1}(\Omega)) \cap H^1(0, T; H^{k+1}(\Omega)) \cap H^3(0, T; L^2(\Omega)) \cap W_4^2(0, T; H^1(\Omega)), \quad (4.1)$$

$$p \in L^\infty(0, T; H^{s+1}(\Omega)), \text{ and } f \in H^2(0, T; L^2(\Omega)). \quad (4.2)$$

For clarity of presentation, we introduce the mesh dependent, nonnegative (energy dissipative) homogeneous weighted functionals

$$\begin{aligned}
\|v\|_{\chi,1}^2 &:= (v - \mathcal{G}_h(w_h^n)v, v), & \|v\|_{\chi,2}^2 &:= (v - \mathcal{G}_h(w_h^n)v, \mathcal{G}_h(w_h^n)v), \\
\|v\|_{\chi,3}^2 &:= (v - \mathcal{G}_h(w_h^n)v, v - \mathcal{G}_h(w_h^n)v).
\end{aligned} \quad (4.3)$$

These are defined on X_h , weighted by the computes w_h^n ; the dependence on w_h^n will be suppressed. For the error between $u(t_n)$ and u_h^n , and $u(t_n)$ and w_h^n , we have the following result.

THEOREM 4.2. *For u , p , and f as described by (4.1), (4.2), satisfying (2.3) - (2.4), and u_h^n , w_h^n given by Algorithm 1.1 we have that, for Δt sufficiently small,*

$$\begin{aligned} \|u - u_h\|_{\infty,0} &\leq \mathcal{F}(\Delta t, h, \chi) + Ch^{k+1} \|u\|_{\infty,k+1} + C\Delta t^2 \|u_{tt}\|_{\infty,0} \\ &\quad + C\left(1 + \frac{\chi}{\Delta t}\right) \left(\Delta t \sum_{j=2}^n [\epsilon(u^j)]^2\right)^{\frac{1}{2}}, \end{aligned} \quad (4.4)$$

$$\|u - w_h\|_{\infty,0} \leq \mathcal{F}(\Delta t, h, \chi) + Ch^{k+1} \|u\|_{\infty,k+1} + C\left(1 + \frac{\chi}{\Delta t}\right) \left(\Delta t \sum_{j=2}^n [\epsilon(u^j)]^2\right)^{\frac{1}{2}}, \quad (4.5)$$

$$\begin{aligned} \chi(1-\chi) \|u(t^n) - w_h^n\|_{\chi,1} + \chi^2 \|u(t^n) - w_h^n\|_{\chi,2} &\leq \mathcal{F}(\Delta t, h, \chi) + Ch^{k+1} \|u\|_{\infty,k+1}, \\ \left(\Delta t \sum_{j=2}^n \left(\Delta t^3 \|D_+ D_- (u^{n-1} - u_h^{n-1})\|^2 + \nu \|\nabla(u^n - w_h^n)\|^2 + \frac{\chi}{\Delta t} \|u^n - w_h^n\|_{\chi,1}^2\right)\right)^{1/2} \\ &\leq \mathcal{F}(\Delta t, h, \chi) + C\left(1 + \frac{\chi}{\Delta t}\right) \left(\Delta t \sum_{j=2}^n [\epsilon(u^j)]^2\right)^{\frac{1}{2}}, \end{aligned}$$

for $2 \leq n \leq N_T$, where

$$\begin{aligned} \mathcal{F}(\Delta t, h, \chi) &:= C\left(\|u^1 - u_h^1\| + \|2(u^1 - u_h^1) - (u^0 - u_h^0)\|\right) \\ &\quad + C\nu^{-1/2} \left(h^{k+1/2} \|u\|_{4,k+1}^2 + h^{k+1/2} \|\nabla u\|_{4,0}^2 + h^{s+1} \|p\|_{2,s+1}\right) \\ &\quad + C\left(h^{k+1} \|u_t\|_{2,k+1} + \nu^{-1} h^k \|u\|_{\infty,k+1} + \frac{\chi}{\Delta t} h^{k+1} \|u\|_{2,k+1} + \Delta t^2 \|u_{ttt}\|_{2,0}\right). \end{aligned}$$

REMARK 4.3 (The regularization error $\epsilon(u)$).

1. For the **nonlinear filter**, the regularization error satisfies

$$\left(\Delta t \sum_{j=2}^n [\epsilon(u^j)]^2\right)^{\frac{1}{2}} \leq C(\delta h^k + h^{k+1} + \delta^2 \min\{\delta^{-1}, \|\nabla \cdot (a(w_h) \nabla u)\|\}) \|u\|_{2,k+1}^2.$$

2. For **approximate deconvolution**, provided $u \in L^\infty(0, T; H^{2N+2}(\Omega))$ for $2N + 2 \geq k + 1$, under the assumption DG1, the regularization error satisfies

$$\left(\Delta t \sum_{j=2}^n [\epsilon(u^j)]^2\right)^{\frac{1}{2}} \leq C(\delta^{2N+2} + \delta h^k + h^{k+1}) (\|u\|_{2,2N+2}^2 + \|u\|_{2,k+1}^2).$$

Proof. [Proof of Theorem 4.2] At time $t^n = n\Delta t$, u given by (2.3)-(2.4) satisfies

$$\begin{aligned} (3u(t^n) - 4u(t^{n-1}) + u(t^{n-2}), v_h) + 2\Delta t \nu (\nabla u(t^n), \nabla v_h) + 2\Delta t b^*(u(t^n), u(t^n), v_h) \\ - 2\Delta t (p(t^n), \nabla \cdot v_h) = 2\Delta t (f(t^n), v_h) + \Delta t \text{Intp}(u^n; v_h), \end{aligned} \quad (4.6)$$

for all $v_h \in V_h$, where $\frac{1}{2} \text{Intp}(u^n; v_h)$ is the local truncation error. Subtracting (1.1) from (4.6), we have for $\varepsilon^n = u(t^n) - w_h^n$, and the pointwise error $e^n = u(t^n) - u_h^n$, (recall that $f^n = f(t^n)$)

$$\begin{aligned} (3\varepsilon^n - 4e^{n-1} + e^{n-2}, v_h) + 2\Delta t \nu (\nabla \varepsilon^n, \nabla v_h) = -2\Delta t b^*(\varepsilon^n, u(t^n), v_h) \\ - 2\Delta t b^*(w_h^n, \varepsilon^n, v_h) + 2\Delta t (p(t^n) - p_h^n, \nabla \cdot v_h) + \Delta t \text{Intp}(u^n; v_h), \end{aligned} \quad (4.7)$$

for all $v_h \in V_h$.

Let $U^n \in V_h$, $\varepsilon^n = u(t^n) - w_h^n = (u(t^n) - U^n) + (U^n - w_h^n) := \Lambda^n + F^n$, and $e^n = u(t^n) - u_h^n = (u(t^n) - U^n) + (U^n - u_h^n) := \Lambda^n + E^n$. With the choice $v_h = F^n$, using $(\nabla \cdot F^n, q_h) = 0, \forall q_h \in Q_h$, and (3.2) we obtain

$$\begin{aligned}
& \frac{1}{2} \|E^n\|^2 + \frac{1}{2} \|2E^n - E^{n-1}\|^2 - \frac{1}{2} \|E^{n-1}\|^2 - \frac{1}{2} \|2E^{n-1} - E^{n-2}\|^2 \\
& \quad + \frac{1}{2} \|E^n - 2E^{n-1} + E^{n-2}\|^2 \\
& + 3(F^n - E^n, F^n) + (3E^n - 4E^{n-1} + E^{n-2}, F^n - E^n) + 2\Delta t \nu \|\nabla F^n\|^2 \\
& = -(3\Lambda^n - 4\Lambda^{n-1} + \Lambda^{n-2}, F^n) - 2\Delta t \nu (\nabla \Lambda^n, \nabla F^n) \\
& \quad - 2\Delta t b^*(\Lambda^n, u(t^n), F^n) - 2\Delta t b^*(F^n, u(t^n), F^n) - 2\Delta t b^*(w_h^n, \Lambda^n, F^n) \\
& \quad + 2\Delta t (p(t^n) - p_h^n - q_h, \nabla \cdot F^n) + \Delta t \text{Int}p(u^n; F^n).
\end{aligned}$$

Summing for $j = 2$ to n yields

$$\begin{aligned}
& \frac{1}{2} \|E^n\|^2 + \frac{1}{2} \|2E^n - E^{n-1}\|^2 + \frac{1}{2} \sum_{j=2}^n \|E^j - 2E^{j-1} + E^{j-2}\|^2 \tag{4.8} \\
& + 3 \sum_{j=2}^n (F^j - E^j, F^j) + \sum_{j=2}^n (3E^j - 4E^{j-1} + E^{j-2}, F^j - E^j) + 2\Delta t \nu \sum_{j=2}^n \|\nabla F^j\|^2 \\
& = \frac{1}{2} \|E^1\|^2 + \frac{1}{2} \|2E^1 - E^0\|^2 - \sum_{j=2}^n (3\Lambda^j - 4\Lambda^{j-1} + \Lambda^{j-2}, F^j) - 2\Delta t \nu \sum_{j=2}^n (\nabla \Lambda^j, \nabla F^j) \\
& \quad - 2\Delta t \sum_{j=2}^n b^*(\Lambda^j, u(t^j), F^j) - 2\Delta t \sum_{j=2}^n b^*(F^j, u(t^j), F^j) - 2\Delta t \sum_{j=2}^n b^*(w_h^j, \Lambda^j, F^j) \\
& \quad + 2\Delta t \sum_{j=2}^n (p(t^j) - p_h^j - q_h, \nabla \cdot F^j) + \Delta t \sum_{j=2}^n \text{Int}p(u^j; F^j).
\end{aligned}$$

Next we estimate the terms on the RHS of (4.8).

$$(3\Lambda^j - 4\Lambda^{j-1} + \Lambda^{j-2}, F^j) = 2\Delta t \left(\frac{3\Lambda^j - 4\Lambda^{j-1} + \Lambda^{j-2}}{2\Delta t}, F^j \right) \tag{4.9}$$

$$\begin{aligned}
& = 2\Delta t (\Lambda_t(t^j), F^j) \leq \Delta t \|\Lambda_t(t^j)\|^2 + \Delta t \|F^j\|^2, \\
& 2\Delta t \nu (\nabla \Lambda^j, \nabla F^j) \leq \Delta t \nu \|\nabla F^j\|^2 + \Delta t \nu \|\nabla \Lambda^j\|^2.
\end{aligned} \tag{4.10}$$

Using $b^*(u, v, w) \leq C(\Omega) \sqrt{\|u\| \|\nabla u\|} \|\nabla v\| \|\nabla w\|$, for $u, v, w \in X$, and Young's inequality, we bound

also

$$\begin{aligned} b^*(\Lambda^j, u(t^j), F^j) &\leq C\sqrt{\|\Lambda^j\| \|\nabla\Lambda^j\|} \|\nabla u(t^j)\| \|\nabla F^j\| \\ &\leq \frac{\nu}{16} \|\nabla F^j\|^2 + C\nu^{-1} \|\Lambda^j\| \|\nabla\Lambda^j\| \|\nabla u(t^j)\|^2, \end{aligned} \quad (4.11)$$

$$\begin{aligned} b^*(F^j, u(t^j), F^j) &\leq C\|F^j\|^{1/2} \|\nabla F^j\|^{3/2} \|\nabla u(t^j)\| \\ &\leq \frac{\nu}{16} \|\nabla F^j\|^2 + C\nu^{-3} \|\nabla u(t^j)\|^4 \|F^j\|^2, \end{aligned} \quad (4.12)$$

$$\begin{aligned} b^*(w_h^j, \Lambda^j, F^j) &\leq C\|\nabla w_h^j\| \|\nabla\Lambda^j\| \|\nabla F^j\| \\ &\leq \frac{\nu}{16} \|\nabla F^j\|^2 + C\nu^{-1} \|\nabla w_h^j\|^2 \|\nabla\Lambda^j\|^2, \end{aligned} \quad (4.13)$$

$$\begin{aligned} (p(t^j) - p_h^j - q_h, \nabla \cdot F^j) &\leq \|p(t^j) - p_h^j - q_h\| \|\nabla \cdot F^j\| \\ &\leq \frac{\nu}{16} \|\nabla F^j\|^2 + C\nu^{-1} \|p(t^j) - p_h^j - q_h\|^2. \end{aligned} \quad (4.14)$$

With the bounds (4.9)-(4.14), (4.8) becomes

$$\begin{aligned} &\frac{1}{2} \|E^n\|^2 + \frac{1}{2} \|2E^n - E^{n-1}\|^2 + \frac{1}{2} \sum_{j=2}^n \|E^j - 2E^{j-1} + E^{j-2}\|^2 \\ &\quad + 3 \sum_{j=2}^n (F^j - E^j, F^j) + \sum_{j=2}^n (3E^j - 4E^{j-1} + E^{j-2}, F^j - E^j) + \frac{\Delta t\nu}{2} \sum_{j=2}^n \|\nabla F^j\|^2 \\ &\leq \frac{1}{2} \|E^1\|^2 + \frac{1}{2} \|2E^1 - E^0\|^2 + \Delta t \sum_{j=2}^n \|\Lambda_t(t^j)\|^2 \\ &\quad + C\Delta t \sum_{j=2}^n (1 + \nu^{-3} \|\nabla u(t^j)\|^4) \|F^j\|^2 + \Delta t\nu \sum_{j=2}^n \|\nabla\Lambda^j\|^2 \\ &\quad + C\nu^{-1} \Delta t \sum_{j=2}^n \|\Lambda^j\| \|\nabla\Lambda^j\| \|\nabla w_h^j\|^2 + C\nu^{-1} \Delta t \sum_{j=2}^n \|\nabla w_h^j\|^2 \|\nabla\Lambda^j\|^2 \\ &\quad + 2C\nu^{-1} \Delta t \sum_{j=2}^n \|p(t^j) - p_h^j - q_h\|^2 + \Delta t \sum_{j=2}^n \text{Intp}(w_h^j; F^j). \end{aligned} \quad (4.15)$$

As u_h^n and w_h^n are connected through Step 2 of Algorithm 1.1, we next use equation (1.2) to obtain a relationship between $\|F^n\|$ and $\|E^n\|$. The true solution $u(\cdot, t^n) = u^n$ satisfies

$$u^n = (1 - \chi)u^n + \chi\mathcal{G}_h(w_h^n)u^n + \chi(u^n - \mathcal{G}_h(w_h^n)u^n). \quad (4.16)$$

Subtracting (1.2) evaluated at n from (4.16) yields

$$e^n = (1 - \chi)\varepsilon^n + \chi\mathcal{G}_h(w_h^n)\varepsilon^n + \chi(u^n - \mathcal{G}_h(w_h^n)u^n), \quad (4.17)$$

and equivalently

$$E^n = (1 - \chi)F^n + \chi\mathcal{G}_h(w_h^n)F^n - \chi(I - \mathcal{G}_h(w_h^n))\Lambda^n + \chi(I - \mathcal{G}_h(w_h^n))u^n. \quad (4.18)$$

Using the assumption (1.3) ($\chi \in [0, 1]$) and (2.10), this implies

$$\|E^n\| \leq \|F^n\| + \chi\|(I - \mathcal{G}_h(w_h^n))\Lambda^n\| + \chi\|(I - \mathcal{G}_h(w_h^n))u^n\|, \quad (4.19)$$

and squaring up and simplifying

$$\begin{aligned} \|E^n\|^2 &\leq \|F^n\|^2 + \Delta t \|F^n\|^2 + 2\chi^2(1 + (\Delta t)^{-1}) \|\Lambda^n - \mathcal{G}_h(w_h^n)\Lambda^n\|^2 \\ &\quad + 2\chi^2(1 + (\Delta t)^{-1}) \|u^n - \mathcal{G}_h(w_h^n)u^n\|^2. \end{aligned} \quad (4.20)$$

Note that by Cauchy-Schwarz inequality we have

$$\frac{1}{2} \|F^n\|^2 + \left(\|F^n\|^2 - \|E^n\|^2 \right) \leq \frac{1}{2} \|E^n\|^2 + 3(F^n - E^n, F^n).$$

Then (4.20) and (4.15) yield

$$\begin{aligned} &\frac{1}{2} \|F^n\|^2 + \frac{1}{2} \|2E^n - E^{n-1}\|^2 + \frac{1}{2} \sum_{j=2}^n \|E^j - 2E^{j-1} + E^{j-2}\|^2 \\ &+ 3 \sum_{j=2}^{n-1} (F^j - E^j, F^j) + \sum_{j=2}^n (3E^j - 4E^{j-1} + E^{j-2}, F^j - E^j) + \frac{\Delta t \nu}{2} \sum_{j=2}^n \|\nabla F^j\|^2 \\ &\leq \Delta t \|F^n\|^2 + 2\chi^2(1 + (\Delta t)^{-1}) \|\Lambda^n - \mathcal{G}_h(w_h^n)\Lambda^n\|^2 + 2\chi^2(1 + (\Delta t)^{-1}) \|u^n - \mathcal{G}_h(w_h^n)u^n\|^2 \\ &\quad + \frac{1}{2} \|E^1\|^2 + \frac{1}{2} \|2E^1 - E^0\|^2 \\ &\quad + \Delta t \sum_{j=2}^n \|\Lambda_t(t^j)\|^2 + C\Delta t \sum_{j=2}^n (1 + \nu^{-3} \|\nabla u(t^j)\|^4) \|F^j\|^2 + \Delta t \nu \sum_{j=2}^n \|\nabla \Lambda^j\|^2 \\ &\quad + 2C\nu^{-1} \Delta t \sum_{j=2}^n \|\Lambda^j\| \|\nabla \Lambda^j\| \|\nabla u^j\|^2 + 2C\nu^{-1} \Delta t \sum_{j=2}^n \|\nabla w_h^j\|^2 \|\nabla \Lambda^j\|^2 \\ &\quad + 2C\nu^{-1} \Delta t \sum_{j=2}^n \|p(t^j) - p_h^j - q_h\|^2 + \Delta t \sum_{j=2}^n \text{Int}p(u^j; F^j). \end{aligned} \quad (4.21)$$

Moreover, (4.18) yields

$$\begin{aligned} F^j - E^j &= \chi(I - \mathcal{G}_h(w_h^n))F^j + \chi(I - \mathcal{G}_h(w_h^n))\Lambda^j - \chi(I - \mathcal{G}_h(w_h^n))u^j \\ 3E^j - 4E^{j-1} + E^{j-2} &= (1 - \chi)(3F^j - 4F^{j-1} + F^{j-2}) \\ &\quad + \chi\mathcal{G}_h(w_h^n)(3F^j - 4F^{j-1} + F^{j-2}) \\ &\quad - \chi(I - \mathcal{G}_h(w_h^n))(3\Lambda^j - 4\Lambda^{j-1} + \Lambda^{j-2}) \\ &\quad + \chi(I - \mathcal{G}_h(w_h^n))(3u^j - 4u^{j-1} + u^{j-2}). \end{aligned}$$

Then using the identity (3.2), Cauchy-Schwarz, assumptions (2.8)-(2.9) ($\|\mathcal{G}_h(w_h^j)\| \leq 1$, $\|I - \mathcal{G}_h(w_h^j)\| \leq$

1), the assumption $\|F^1\| = \|2F^1 - F^0\| = 0$, the Minkowski inequality yields

$$\begin{aligned}
& 3 \sum_{j=2}^{n-1} (F^j - E^j, F^j) + \sum_{j=2}^n (3E^j - 4E^{j-1} + E^{j-2}, F^j - E^j) \\
& \geq \mathcal{C}_{1,\chi,T} - \frac{\chi^2}{2} \|\Lambda^n\|_{\chi,3}^2 - \frac{1}{2} \chi^2 \|2\Lambda^n - \Lambda^{n-1}\|_{\chi,3}^2 \\
& \quad - \frac{\chi^2}{2} \|u^n\|_{\chi,3}^2 - \frac{1}{2} \chi^2 \|2u^n - u^{n-1}\|_{\chi,3}^2 - \frac{\chi^2}{2} \|u^n - 2u^{n-1} + u^{n-2}\|_{\chi,3}^2 \\
& \quad - \Delta t \sum_{j=0}^n \|F^j\|^2 - C \frac{\chi^2}{\Delta t} (1 + \chi) \sum_{j=2}^n \|(I - \mathcal{G}_h(w_h^j))\Lambda^j\|^2 \\
& \quad - C \Delta t \left(1 + \chi + \frac{\chi^2}{(\Delta t)^2} + \frac{\chi^3}{(\Delta t)^2} + \frac{\chi^4}{(\Delta t)^2} \right) \sum_{j=2}^n \|(I - \mathcal{G}_h(w_h^j))u^j\|^2 \tag{4.22}
\end{aligned}$$

where

$$\mathcal{C}_{1,\chi,T} = 3\chi \sum_{j=2}^{n-1} \|F^j\|_{\chi,1}^2 + \frac{(1-\chi)\chi}{2} \|F^n\|_{\chi,1}^2 + \frac{\chi^2}{2} \|F^n\|_{\chi,2}^2.$$

From (4.22) and (4.21) we obtain (use $\chi \in [0, 1]$, $\Delta t < 1$, (2.7), (2.10))

$$\begin{aligned}
& \frac{1}{2} \|F^n\|^2 + \mathcal{C}_T + \frac{\Delta t \nu}{2} \sum_{j=2}^n \|\nabla F^j\|^2 \tag{4.23} \\
& \leq \mathcal{C}_0 + C \chi^2 (\Delta t)^{-1} \sum_{j=2}^n \|\Lambda^j\|^2 + C (1 + \chi^2 (\Delta t)^{-2}) \Delta t \sum_{j=2}^n [\epsilon(u^j)]^2 \\
& \quad + \Delta t \sum_{j=2}^n \|\Lambda_t(t^j)\|^2 + C \Delta t \sum_{j=0}^n (1 + \nu^{-3} \|\nabla u(t^j)\|^4) \|F^j\|^2 + \Delta t \nu \sum_{j=2}^n \|\nabla \Lambda^j\|^2 \\
& \quad + C \nu^{-1} \Delta t \sum_{j=2}^n \|\Lambda^j\| \|\nabla \Lambda^j\| \|\nabla u^j\|^2 + C \nu^{-1} \Delta t \sum_{j=2}^n \|\nabla w_h^j\|^2 \|\nabla \Lambda^j\|^2 \\
& \quad + C \nu^{-1} \Delta t \sum_{j=2}^n \|p(t^j) - p_h^j - q_h\|^2 + \Delta t \sum_{j=2}^n \text{Intp}(u^j; F^j),
\end{aligned}$$

where

$$\begin{aligned}
\mathcal{C}_0 &= \frac{1}{2} \|E^1\|^2 + \frac{1}{2} \|2E^1 - E^0\|^2 \\
\mathcal{C}_T &= 3\chi \sum_{j=2}^{n-1} \|F^j\|_{\chi,1}^2 + \frac{(1-\chi)\chi}{2} \|F^n\|_{\chi,1}^2 \\
& \quad + \frac{\chi^2}{2} \|F^n\|_{\chi,2}^2 + \frac{1}{2} \|2E^n - E^{n-1}\|^2 + \frac{1}{2} \sum_{j=2}^n \|E^j - 2E^{j-1} + E^{j-2}\|^2.
\end{aligned}$$

The terms on the RHS of (4.23) can be further simplified as follows.

$$C \frac{\chi^2}{\Delta t} \sum_{j=2}^n \|\Lambda^j\|^2 \leq C \frac{\chi^2}{\Delta t} \sum_{j=2}^n h^{2k+2} |u^j|_{k+1}^2 \leq C \chi^2 (\Delta t)^{-2} h^{2k+2} \|u\|_{2,k+1}^2, \quad (4.24)$$

$$\nu \Delta t \sum_{j=2}^n \|\nabla \Lambda^j\|^2 \leq C \nu \Delta t \sum_{j=2}^n h^{2k} |u^j|_{k+1}^2 \leq C \nu h^{2k} \|u\|_{2,k+1}^2. \quad (4.25)$$

For the next term

$$\begin{aligned} C \nu^{-1} \Delta t \sum_{j=2}^n \|\nabla w^j\|^2 \|\Lambda^j\| \|\nabla \Lambda^j\| &\leq C \nu^{-1} h^{2k+1} \Delta t \sum_{j=2}^n |u^j|_{k+1}^2 \|\nabla w^j\|^2 \\ &\leq C \nu^{-1} h^{2k+1} \Delta t \left(\sum_{j=2}^n |u^j|_{k+1}^4 + \sum_{j=2}^n \|\nabla w^j\|^4 \right) \leq C \nu^{-1} h^{2k+1} (\|u\|_{4,k+1}^4 + \|\nabla u\|_{4,0}^4). \end{aligned} \quad (4.26)$$

Using the boundedness of $\nu \Delta t \sum_{j=2}^n \|\nabla w_h^j\|$ (Proposition 3.3)

$$C \nu^{-1} \Delta t \sum_{j=2}^n \|\nabla w_h^j\|^2 \|\nabla \Lambda^j\|^2 \leq C \nu^{-2} h^{2k} \|u\|_{\infty,k+1}^2. \quad (4.27)$$

Next

$$\begin{aligned} \Delta t \sum_{j=2}^n \|\Lambda_t(t^j)\|^2 &\leq \Delta t \sum_{j=2}^n h^{2k+2} \|u_t(t^j)\|_{k+1}^2 \leq h^{2k+2} \|u_t\|_{2,k+1}^2. \\ \nu^{-1} \Delta t \sum_{j=2}^n \|p(t^j) - p_h^j - q_h\|^2 &\leq \nu^{-1} \Delta t \sum_{n=1}^l h^{2s+2} \|p(t^j)\|_{s+1}^2 \leq C \nu^{-1} h^{2s+2} \|p\|_{2,s+1}^2. \end{aligned} \quad (4.28)$$

As in [21] the *interpolation error* in (4.23) can be bounded as

$$\Delta t \sum_{j=2}^n |Intp(u^n; F^n)| \leq \Delta t \sum_{j=2}^n \|F^j\|^2 + C (\Delta t)^4 \|u_{ttt}\|_{2,0}^2. \quad (4.29)$$

Combining (4.25)–(4.29), the inequality (4.23) simplifies to

$$\begin{aligned} &\frac{1}{2} \|F^n\|^2 + \mathcal{C}_T + \frac{\Delta t \nu}{2} \sum_{j=2}^n \|\nabla F^j\|^2 \\ &\leq \mathcal{C}_0 + C \Delta t \sum_{j=2}^n \left(1 + \nu^{-3} \|\nabla u(t^j)\|^4 \right) \|F^j\|^2 + h^{2k+2} \|u_t\|_{2,k+1}^2 + C \nu h^{2k} \|u\|_{2,k+1}^2 \\ &\quad + C \nu^{-1} h^{2k+1} \left(\|u\|_{4,k+1}^4 + \|\nabla u\|_{4,0}^4 \right) + C \nu^{-2} h^{2k} \|u\|_{\infty,k+1}^2 \\ &\quad + C \nu^{-1} h^{2s+2} \|p\|_{2,s+1}^2 + C \chi^2 (\Delta t)^{-2} h^{2k+2} \|u\|_{2,k+1}^2 \\ &\quad + C (1 + \chi^2 (\Delta t)^{-2}) \Delta t \sum_{j=2}^n [\epsilon(u^j)]^2 + C (\Delta t)^4 \|u_{ttt}\|_{2,0}^2. \end{aligned} \quad (4.30)$$

Hence, with Δt sufficiently small, i.e. $\Delta t < C(1 + \nu^{-3} \|\nabla u\|_{\infty,0}^4)^{-1}$, from the discrete Gronwall's Lemma [24], we have

$$\begin{aligned}
& \|F^n\|^2 + (1 - \chi)\chi \|F^n\|_{\chi,1}^2 + \chi^2 \|F^n\|_{\chi,2}^2 + \frac{\chi}{\Delta t} \Delta t \sum_{j=2}^n \|F^j\|_{\chi,1}^2 \\
& + \|2E^n - E^{n-1}\|^2 + \Delta t \sum_{j=2}^n \Delta t^3 \left\| \frac{E^j - 2E^{j-1} + E^{j-2}}{\Delta t^2} \right\|^2 + \Delta t \nu \sum_{j=2}^n \|\nabla F^j\|^2 \\
& \leq C \left(\|E^1\|^2 + \|2E^1 - E^0\|^2 \right) \\
& + Ch^{2k+2} \|u_t\|_{2,k+1}^2 + C\nu h^{2k} \|u\|_{2,k+1}^2 + C\nu^{-1} h^{2k+1} \left(\|u\|_{4,k+1}^4 + \|\nabla u\|_{4,0}^4 \right) \\
& + C\nu^{-2} h^{2k} \|u\|_{\infty,k+1}^2 + C\nu^{-1} h^{2s+2} \|p\|_{2,s+1}^2 + C\chi^2 (\Delta t)^{-2} h^{2k+2} \|u\|_{2,k+1}^2 \\
& + C(1 + \chi^2 (\Delta t)^{-2}) \Delta t \sum_{j=2}^n [\epsilon(u^j)]^2 + C(\Delta t)^4 \|u_{ttt}\|_{2,0}^2.
\end{aligned} \tag{4.31}$$

The estimate given in (4.5) for $\|u - w_h\|_{\infty,0}$ then follows from the triangle inequality, Lemma 2.9 and (4.31). The estimate for $\|u - u_h\|_{\infty,0}$ follows similarly, after noting the extrapolation

$$\square \quad \|E^{n+1}\| \leq \|2E^n - E^{n-1}\| + C\Delta t^2 \|E_{tt}^{n+1}\|.$$

For the case of Taylor-Hood approximating elements, i.e. $k = 2, s = 1$, we have the following asymptotic estimate.

COROLLARY 4.4. *Under the assumptions of Theorem 4.2, with $\delta = Ch$ and (X_h, Q_h) given by the Taylor-Hood approximation elements, we have*

$$\begin{aligned}
& \|u - w_h\|_{\infty,0} + \|u - u_h\|_{\infty,0} \\
& + \left[\Delta t \sum_{j=2}^n \left(\Delta t^3 \|D_+ D_-(u^n - u_h^n)\|^2 + \nu \|\nabla(u^n - w_h^n)\|^2 + \frac{\chi}{\Delta t} \|u^n - w_h^n\|_{\chi,1}^2 \right) \right]^{1/2} \\
& \leq C(u, p, \nu) \left\{ \Delta t^2 + h^2 + \frac{h^3}{\Delta t} + \frac{\chi}{\Delta t} \left(\Delta t \sum_{j=2}^n [\epsilon(u^j)]^2 \right)^{\frac{1}{2}} \right\}.
\end{aligned} \tag{4.32}$$

The increase in stability involves the functional $\|\cdot\|_{\chi,1}$, defined in (4.3). This functional has the property of measuring high frequency components of a function, while diminishing the influence of low frequency components. For the two approximations u_h and w_h we have the following estimates. Estimate (4.33) shows that the high frequency components of w_h^n , typically spurious oscillations, are diminished in forming u_h^n , i.e., $\|u_h^n\|_{\chi,1} < \|w_h^n\|_{\chi,1}$. The second estimate (4.34) establishes a relationship between the high frequency components of the error in u_h^n and w_h^n , i.e. $\|u^n - u_h^n\|_{\chi,1}$ and $\|u^n - w_h^n\|_{\chi,1}$, respectively. Note that taking $\phi := (I - \mathcal{G}_h(w_h^n))v$ in assumptions (2.8)-(2.10) we obtain

$$((I - \mathcal{G}_h(w_h^n))v, (I - \mathcal{G}_h(w_h^n))\mathcal{G}_h(w_h^n)v) \geq 0 \quad \forall v \in V_h.$$

THEOREM 4.5. *Under the assumptions of Theorem 4.2, for $n = 1, 2, \dots, N_T, 0 \leq \delta \leq 1$,*

$$\|u_h^n\|_{\chi,1}^2 = \|w_h^n\|_{\chi,1}^2 - \chi(2 - \chi) \|w_h^n\|_{\chi,3}^2 - \chi^2 (w_h^n - \mathcal{G}_h(w_h^n)w_h^n, (I - \mathcal{G}_h(w_h^n))\mathcal{G}_h(w_h^n)w_h^n), \tag{4.33}$$

$$\begin{aligned}
& \|u^n - u_h^n\|_{\chi,1}^2 \leq \|u^n - w_h^n\|_{\chi,1}^2 - \chi^2 ((I - \mathcal{G}_h(w_h^n))(u^n - w_h^n), (I - \mathcal{G}_h(w_h^n))\mathcal{G}_h(w_h^n)(u^n - w_h^n)) \\
& - \frac{3}{2}\chi(1 - \chi) \|u^n - w_h^n\|_{\chi,3}^2 + 2\chi(1 + \chi) \|u^n\|_{\chi,3}^2 + \chi^2 \|(I - \mathcal{G}_h(w_h^n))u^n\|_{\chi,1}^2.
\end{aligned} \tag{4.34}$$

Proof. Taking the inner product of both sides of (1.2) at level n with $u_h^n - \mathcal{G}_h(w_h^n)u_h^n$, we obtain

$$\begin{aligned}
& \# u_h^n \#_{\chi,1}^2 = (u_h^n, (I - \mathcal{G}_h(w_h^n))u_h^n) \\
& = \left(w_h^n - \chi(I - \mathcal{G}_h(w_h^n))w_h^n, (I - \mathcal{G}_h(w_h^n))[w_h^n - \chi(I - D_h G_h)w_h^n] \right) \\
& = \# w_h^n \#_{\chi,1}^2 + \chi^2 \left((I - \mathcal{G}_h(w_h^n))w_h^n, (I - \mathcal{G}_h(w_h^n))^2 w_h^n \right) - \chi \left(w_h^n, (I - \mathcal{G}_h(w_h^n))^2 w_h^n \right) \\
& \quad - \chi \left((I - \mathcal{G}_h(w_h^n))w_h^n, (I - \mathcal{G}_h(w_h^n))w_h^n \right) \\
& = \# w_h^n \#_{\chi,1}^2 + \chi^2 \|w_h^n\|_{\chi,3}^2 - \chi^2 \left((I - \mathcal{G}_h(w_h^n))w_h^n, (I - \mathcal{G}_h(w_h^n))\mathcal{G}_h(w_h^n)w_h^n \right) - 2\chi \|w_h^n\|_{\chi,3}^2 \\
& = \# w_h^n \#_{\chi,1}^2 - \chi(2 - \chi) \|w_h^n\|_{\chi,3}^2 - \chi^2 \left((I - \mathcal{G}_h(w_h^n))w_h^n, (I - \mathcal{G}_h(w_h^n))\mathcal{G}_h(w_h^n)w_h^n \right),
\end{aligned}$$

which establishes (4.33).

To establish (4.34) we begin with (4.17). Taking the inner product of both sides with $\varepsilon^n - \mathcal{G}_h(w_h^n)\varepsilon^n$,

$$(e^n, (I - \mathcal{G}_h(w_h^n))\varepsilon^n) = \# \varepsilon^n \#_{\chi,1}^2 - \chi \|\varepsilon^n\|_{\chi,3}^2 + \chi \left((I - \mathcal{G}_h(w_h^n))u^n, (I - \mathcal{G}_h(w_h^n))\varepsilon^n \right),$$

and by the polarization identity

$$\begin{aligned}
& \frac{1}{2} \# e^n \#_{\chi,1}^2 + \frac{1}{2} \# \varepsilon^n \#_{\chi,1}^2 - \frac{1}{2} \# e^n - \varepsilon^n \#_{\chi,1}^2 \\
& = \# \varepsilon^n \#_{\chi,1}^2 - \chi \|\varepsilon^n\|_{\chi,3}^2 + \chi \left((I - \mathcal{G}_h(w_h^n))u^n, (I - \mathcal{G}_h(w_h^n))\varepsilon^n \right).
\end{aligned}$$

Thus,

$$\# \varepsilon^n \#_{\chi,1}^2 = \# e^n \#_{\chi,1}^2 - \# e^n - \varepsilon^n \#_{\chi,1}^2 + 2\chi \|\varepsilon^n\|_{\chi,3}^2 - 2\chi \left((I - \mathcal{G}_h(w_h^n))u^n, (I - \mathcal{G}_h(w_h^n))\varepsilon^n \right). \quad (4.35)$$

In addition, rearranging (4.18) we have

$$e^n - \varepsilon^n = -\chi(I - \mathcal{G}_h(w_h^n))\varepsilon^n + \chi(I - \mathcal{G}_h(w_h^n))u^n$$

and thus,

$$\begin{aligned}
& \# e^n - \varepsilon^n \#_{\chi,1}^2 = \left((e^n - \varepsilon^n), (I - \mathcal{G}_h(w_h^n))(e^n - \varepsilon^n) \right) \\
& = \chi^2 \# (I - \mathcal{G}_h(w_h^n))\varepsilon^n \#_{\chi,1}^2 + \chi^2 \# (I - \mathcal{G}_h(w_h^n))u^n \#_{\chi,1}^2 \\
& \quad - \chi^2 \left((I - \mathcal{G}_h(w_h^n))\varepsilon^n, (I - \mathcal{G}_h(w_h^n))^2 u^n \right) - \chi^2 \left((I - \mathcal{G}_h(w_h^n))u^n, (I - \mathcal{G}_h(w_h^n))^2 \varepsilon^n \right).
\end{aligned} \quad (4.36)$$

Substituting (4.36) into (4.35) and rearranging

$$\begin{aligned}
\# \varepsilon^n \#_{\chi,1}^2 & = \# e^n \#_{\chi,1}^2 - \chi^2 \# (I - \mathcal{G}_h(w_h^n))\varepsilon^n \#_{\chi,1}^2 - \chi^2 \# (I - \mathcal{G}_h(w_h^n))u^n \#_{\chi,1}^2 \\
& \quad + \chi^2 \left((I - \mathcal{G}_h(w_h^n))\varepsilon^n, (I - \mathcal{G}_h(w_h^n))^2 u^n \right) + \chi^2 \left((I - \mathcal{G}_h(w_h^n))u^n, (I - \mathcal{G}_h(w_h^n))^2 \varepsilon^n \right) \\
& \quad + 2\chi \|\varepsilon^n\|_{\chi,3}^2 - 2\chi \left((I - \mathcal{G}_h(w_h^n))u^n, (I - \mathcal{G}_h(w_h^n))\varepsilon^n \right).
\end{aligned} \quad (4.37)$$

Note that

$$\begin{aligned}
& -\chi^2 \# (I - \mathcal{G}_h(w_h^n))\varepsilon^n \#_{\chi,1}^2 + 2\chi \|\varepsilon^n\|_{\chi,3}^2 \\
& = (2\chi - \chi^2) \|\varepsilon^n\|_{\chi,3}^2 + \chi^2 \left((I - \mathcal{G}_h(w_h^n))\varepsilon^n, \mathcal{G}_h(w_h^n)(I - \mathcal{G}_h(w_h^n))\varepsilon^n \right),
\end{aligned} \quad (4.38)$$

$$\chi^2 \left((I - \mathcal{G}_h(w_h^n))\varepsilon^n, (I - \mathcal{G}_h(w_h^n))^2 u^n \right) \leq \frac{\chi^2}{4} \|\varepsilon^n\|_{\chi,3}^2 + \chi^2 \|(I - \mathcal{G}_h(w_h^n))u^n\|_{\chi,3}^2, \quad (4.39)$$

$$\chi^2((I - \mathcal{G}_h(w_h^n))u^n, (I - \mathcal{G}_h(w_h^n))^2\varepsilon^n) \leq \chi^2\|u^n\|_{\chi,3}^2 + \frac{\chi^2}{4}\|(I - \mathcal{G}_h(w_h^n))\varepsilon^n\|_{\chi,3}^2, \quad (4.40)$$

$$2\chi((I - \mathcal{G}_h(w_h^n))u^n, (I - \mathcal{G}_h(w_h^n))\varepsilon^n) \leq \frac{1}{2}\chi\|\varepsilon^n\|_{\chi,3}^2 + 2\chi\|u^n\|_{\chi,3}^2. \quad (4.41)$$

Thus, using (4.38)-(4.41) in (4.37), we obtain

$$\begin{aligned} \|\varepsilon^n\|_{\chi,1}^2 &\geq \|e^n\|_{\chi,1}^2 + \frac{3}{2}\chi(1-\chi)\|\varepsilon^n\|_{\chi,3}^2 + \chi^2((I - \mathcal{G}_h(w_h^n))\varepsilon^n, \mathcal{G}_h(w_h^n)(I - \mathcal{G}_h(w_h^n))\varepsilon^n) \\ &\quad - 2\chi(1+\chi)\|u^n\|_{\chi,3}^2 - \chi^2\|(I - \mathcal{G}_h(w_h^n))u^n\|_{\chi,1}^2. \end{aligned}$$

□

5. Numerical Experiments. In this section we present four numerical experiments. Using the Green-Taylor vortex problem and selecting regularization by deconvolution $G_h(\phi) = D_h^N(\bar{\phi})$, we confirm the predicted convergence rates and compare the accuracy for deconvolution orders $N = 0, 1, 2$. We then consider the flow around a cylinder and Poiseuille benchmark problems and rotating flow between offset cylinders.

We use *FreeFEM++* [23] to run the numerical tests. Algorithm 1.1 is discretized in space using Taylor-Hood elements (continuous piecewise quadratic polynomials for the velocity and continuous linears for the pressure). The nonlinear system at each time step was solved by a fixed point iteration. The Stokes filter and van Cittert deconvolution of orders $N = 0, 1$ or 2 were used in all the computations. It was applied with the same boundary conditions as given for the problem being solved.

m	$\ u - u_h\ _{\infty,0}$	rate	$\ \nabla u - \nabla u_h\ _{2,0}$	rate
16	$2.74021 \cdot 10^{-2}$		$1.64089 \cdot 10^{-1}$	
32	$2.61947 \cdot 10^{-2}$	0.06	$1.50942 \cdot 10^{-1}$	0.12
48	$2.42064 \cdot 10^{-2}$	0.19	$1.3133 \cdot 10^{-1}$	0.34
64	$2.12955 \cdot 10^{-2}$	0.45	$1.09657 \cdot 10^{-1}$	0.63
80	$1.78571 \cdot 10^{-2}$	0.79	$9.03406 \cdot 10^{-2}$	0.87
96	$1.47115 \cdot 10^{-2}$	1.06	$7.46497 \cdot 10^{-2}$	1.05

Table 5.1: Poor convergence without relaxation or deconvolution.

m	$\ u - u_h\ _{\infty,0}$	rate	$\ \nabla u - \nabla u_h\ _{2,0}$	rate
16	$2.60813 \cdot 10^{-2}$		$1.52619 \cdot 10^{-1}$	
32	$1.4652 \cdot 10^{-2}$	0.83	$8.08192 \cdot 10^{-2}$	0.96
48	$5.61527 \cdot 10^{-3}$	2.37	$4.03054 \cdot 10^{-2}$	1.72
64	$2.49971 \cdot 10^{-3}$	2.81	$2.29939 \cdot 10^{-2}$	1.95
80	$1.27253 \cdot 10^{-3}$	3.03	$1.44953 \cdot 10^{-2}$	2.07
96	$7.14506 \cdot 10^{-4}$	3.17	$9.88172 \cdot 10^{-3}$	2.10

Table 5.2: Errors and convergence rates for deconvolution $N = 1, \chi = 0$.

5.1. Convergence Rate Verification. Our first test is designed to test (and does confirm) the predicted rates of convergence. The problem of simulating decay of the Green-Taylor vortex, [46, 45],

m	$\ u - u_h\ _{\infty,0}$	rate	$\ \nabla u - \nabla u_h\ _{2,0}$	rate
16	$1.00069 \cdot 10^{-3}$		$1.61231 \cdot 10^{-2}$	
32	$1.48731 \cdot 10^{-4}$	2.75	$2.62388 \cdot 10^{-3}$	2.62
48	$4.19167 \cdot 10^{-5}$	3.12	$9.44449 \cdot 10^{-4}$	2.52
64	$1.63416 \cdot 10^{-5}$	3.27	$4.71362 \cdot 10^{-4}$	2.42
80	$7.71333 \cdot 10^{-6}$	3.36	$2.8071 \cdot 10^{-4}$	2.32
96	$4.12874 \cdot 10^{-6}$	3.43	$1.86365 \cdot 10^{-4}$	2.25

Table 5.3: Errors and convergence rates for deconvolution $N = 1$ with $\chi = \Delta t$.

m	$\ u - u_h\ _{\infty,0}$	rate	$\ \nabla u - \nabla u_h\ _{2,0}$	rate
16	$4.98747 \cdot 10^{-4}$		$1.54581 \cdot 10^{-2}$	
32	$4.63728 \cdot 10^{-5}$	3.43	$2.38295 \cdot 10^{-3}$	2.70
48	$1.0654 \cdot 10^{-5}$	3.63	$8.57864 \cdot 10^{-4}$	2.52
64	$3.66425 \cdot 10^{-6}$	3.71	$4.34974 \cdot 10^{-4}$	2.36
80	$1.59044 \cdot 10^{-6}$	3.74	$2.6326 \cdot 10^{-4}$	2.25
96	$8.04969 \cdot 10^{-7}$	3.73	$1.77074 \cdot 10^{-4}$	2.18

Table 5.4: Errors and convergence rates for deconvolution $N = 2$ with $\chi = \Delta t$.

is an interesting test problem in which the true solution is known (which is required to compute the errors to obtain rates of convergence). It is a commonly used test for accuracy experiments, e.g., [11, 44, 26]. For an insightful analysis see [5] and [7]. The prescribed solution in $\Omega = (0, 1) \times (0, 1)$ is given by

$$\begin{aligned}
u_1(x, y, t) &= -\cos(\omega\pi x) \sin(\omega\pi y) e^{-2\omega^2\pi^2 t/\tau}, \\
u_2(x, y, t) &= \sin(\omega\pi x) \cos(\omega\pi y) e^{-2\omega^2\pi^2 t/\tau}, \\
p(x, y, t) &= -\frac{1}{4}(\cos(2\omega\pi x) + \cos(2\omega\pi y)) e^{-2\omega^2\pi^2 t/\tau}.
\end{aligned}$$

When $\tau = Re$, this is a solution of the NSE with $f = 0$, consisting of an $\omega \times \omega$ array of oppositely signed vortices that decay as $t \rightarrow \infty$.

In our tests we choose $\omega = 1$, $T = 1$, Reynolds number $Re = 100$ and $\delta = h = 1/m$, the interval $(0, 1)$. The results for Algorithm 1.1 are presented in Table 5.2, using order of deconvolution $N = 1$ without relaxation (i.e. $\chi = 0$). Tables 5.3 and 5.4 present the results for $N = 1$ and $N = 2$ with relaxation for $\chi = \Delta t$, respectively. Results using the simple averaging filter, i.e. deconvolution with order $N = 0$ and $\chi = 0$, are presented in Table 5.1. The convergence rate is calculated from the error at two successive values of h in the usual manner by postulating $e(h) = Ch^\beta$ and solving for β via $\beta = \ln(e(h_1)/e(h_2))/\ln(h_1/h_2)$.

From the tables we see the convergence rate approaches the second order rate predicted for $\|\nabla u - \nabla u_h\|_{2,0}$ and we also see what appears to be an L^2 lift for $\|u - u_h\|_{\infty,0}$ for order of deconvolution $N = 1$ and $N = 2$. The method with the simple averaging filter, order of deconvolution $N = 0$, has much larger errors and slower rates of convergence, as expected. From this test it is clear that (i) *relaxation is important to control the loss of accuracy due to blow up of the numerical dissipation as $\Delta t \rightarrow 0$* , and (ii) *regularization using filtering plus deconvolution is superior to filtering alone*, as predicted in Theorem 4.2.

5.2. Flow around a cylinder. Our next numerical illustration is for two dimensional *under-resolved* flow around a cylinder. Thus, our goal is not to use a fine mesh and reproduce the benchmark

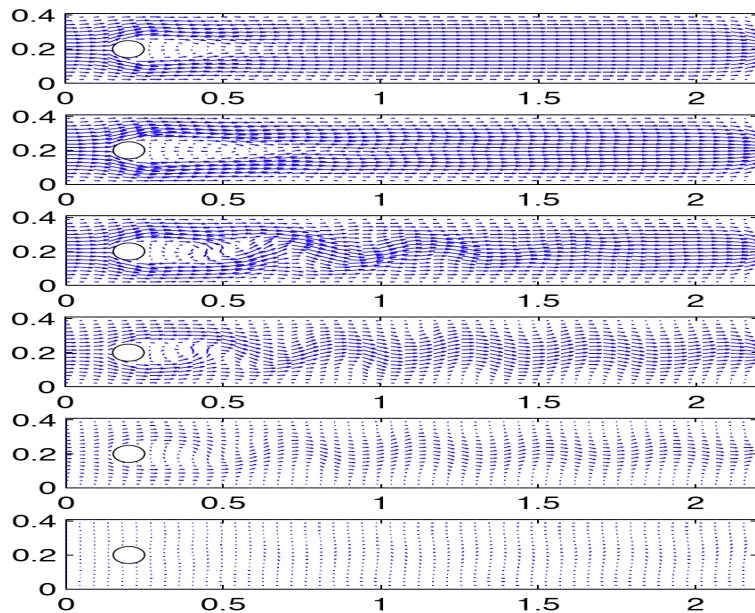


Fig. 5.1: The velocity at $t = 2, 4, 5, 6, 7,$ and 8 of Algorithm 1.1, with $N = 1$ and $\chi = \Delta t = 0.005$.

values from [37, 25] but rather to see how close to those values we can come on a mesh coarse enough that accuracy cannot be reasonably expected. We compute values for the maximal drag $c_{d,max}$ and lift $c_{l,max}$ coefficient at the cylinder, and for the pressure difference $\Delta p(t)$ between the front and back of the cylinder at the final time $T = 8$. It is not turbulent but does have interesting features. The flow patterns are driven by the interaction of a fluid with a wall which is an important scenario for industrial flows. This flow is actually quite difficult to simulate successfully by a model with sufficient regularization to handle higher Reynolds number problems.

The time dependent inflow profile is

$$u_1(0, y, t) = u_1(2.2, y, t) = \frac{6}{0.41^2} \sin(\pi t/8) y(0.41 - y),$$

$$u_2(0, y, t) = u_2(2.2, y, t) = 0.$$

No slip boundary conditions are prescribed along the top and bottom walls, "do-nothing" at the outflow, and the initial condition is $u(x, y, 0) = 0$. The viscosity is $\nu = 10^{-3}$ and the external force $f = 0$. The Reynolds number of the flow, based on the diameter of the cylinder and on the mean velocity inflow is $0 \leq Re \leq 100$. A mesh with 62757 number of degrees of freedom is used for all simulation for a clear comparison of the different parameter settings presented in this report. The filter radius is chosen as the perimeter of the cylinder divided by the number of mesh points around the cylinder.

From time $t = 2$ to $t = 4$ two vortices start to develop behind the cylinder. Between $t = 4$ and $t = 5$, the vortices separate from the cylinder, so that a vortex street develops, and they continue to be visible through the final time $t = 8$. This can be seen in Figure 5.1. The evolutions of $c_{d,max}$, $c_{l,max}$ and Δp are presented in Figure 5.2.

For the computation of drag and lift coefficients we used the one dimensional method described by John [25]. Results on the computations of maximal drag and lift coefficients and pressure drop,

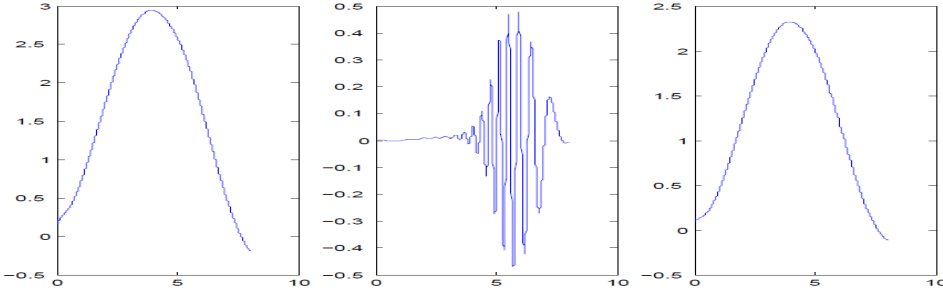


Fig. 5.2: The development of $c_d(t)$, $c_l(t)$ and $\Delta p(t)$ of Algorithm 1.1 with $N = 1$ and $\chi = \Delta t = 0.005$.

for $N = 1$, are presented in Table 5.5. The following reference intervals are given in [37]

$$c_{d,max}^{ref} \in [2.93, 2.97], \quad c_{l,max}^{ref} \in [0.47, 0.49], \quad \Delta p^{ref} \in [-0.115, -0.105]$$

and also the following reference values are given in [25]

$$\begin{aligned} t(c_{d,max}^{ref}) &= 3.93625, & c_{d,max}^{ref} &= 2.950921575 \\ t(c_{l,max}^{ref}) &= 5.693125, & c_{l,max}^{ref} &= 0.47795 \\ \Delta p^{ref}(8s) &= -0.1116 \end{aligned}$$

relax. coeff.	Δt	$t(c_{d,max})$	$c_{d,max}$	$t(c_{l,max})$	$c_{l,max}$	$\Delta p(8s)$
$\chi = 0$	0.02	3.94	2.81978	6.14	0.320677	-0.109436
	0.01	3.93	2.75983	6.02	0.366276	-0.0996473
	0.005	3.925	2.66524	6.03	0.325459	-0.098704
$\chi = \Delta t$	0.02	3.94	2.94149	6.12	0.360383	-0.106385
	0.01	3.93	2.94231	5.96	0.454216	-0.108634
	0.005	3.935	2.94268	5.925	0.477011	-0.111908

Table 5.5: Drag/lift coefficients and pressure difference for $N = 1$ deconvolution.

Table 5.5 shows that using a regularization operator in Step 2 of Algorithm 1.1 works well in combination with the BDF2 time discretization in Algorithm 1.1. It computes the drag and lift coefficients, and the pressure difference, within the benchmark intervals, and illustrates the positive role of using relaxation in the approximation algorithm.

5.3. Poiseuille Flow. A discussion of this problem can be found in Canuto, Hussaini, Quarteroni, and Zang [10]. The goal of this test is to test the contribution of the BDF2 discretization in Step 1 by comparing the sensitivity to perturbations over longer time intervals and higher Re of Algorithm 1.1 to Algorithm 1.1 with Step 1 replaced by the CN method, studied in [18]. To do so we initialize with a linearly stable equilibrium solution and take many steps with a large Δt to check for deviations from equilibrium. At each time step there are small perturbations due to discretization effects. Thus we test if this linearly stable flow remains linearly stable under CN versus BDF2 methods used in Step 1 of Algorithm 1.1.

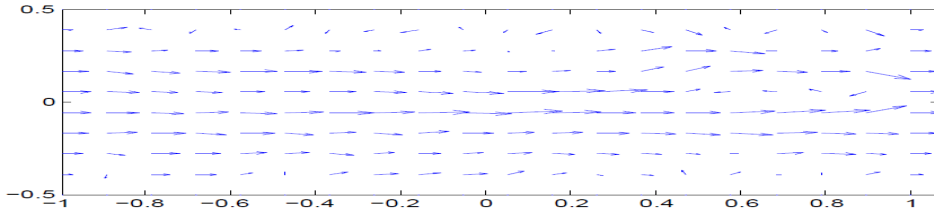


Fig. 5.3: Incorrect velocity field when Step 1 uses Crank-Nicolson.

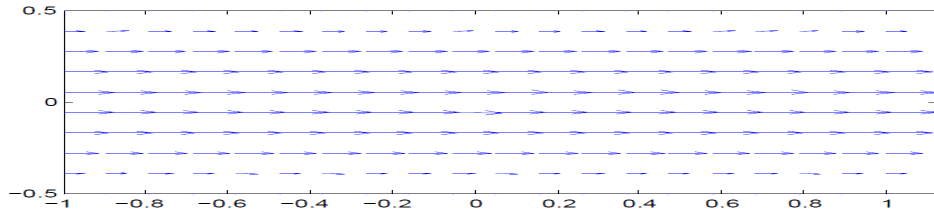


Fig. 5.4: Correct velocity field when Step 1 uses BDF2.

The results show that BDF2 increases the stability of Algorithm 1.1 over the CN time discretization. In $\Omega = (-1, 1) \times (-0.5, 0.5)$, a parabolic velocity $v(x, t) = 0$ and $u(x, y, t) = (y + 0.5) * (0.5 - y)$ is prescribed at the inflow and outflow. No-slip boundary conditions are given at the top and bottom. The exact solution is well known to be $v(x, y) = 0, u(x, y) = (y + 0.5) * (0.5 - y), p(x, y) = -2\nu x$, and we take it as our initial condition. We take the viscosity $\nu = 10^{-5}$, filter width $\delta = 0.1$, order of deconvolution $N = 1$ and relaxation parameter $\chi = \Delta t$. A uniform mesh consisting of triangles with 1953 number of degrees of freedom was used.

For time step $\Delta t = 1$, the results of the velocity fields after 123 time steps show that Algorithm 1.1 is both more accurate and more stable. At $T = 123$ using CN in Algorithm 1.1 the flow lost its features, see Figure 5.3, while the velocity field computed by the Algorithm 1.1 is properly simulated even at $T = 200$, see Figure 5.4.

Relative velocity errors for the given initial condition with time step $\Delta t = 0.5$ and 1 and relative velocity errors for a perturbed initial condition $v(x, y) = 0, u(x, y) = (y + 0.5)(0.5 - y) + 0.001 \sin(4\pi y)$ with time step $\Delta t = 0.5$ and 1 are given in Figure 5.5 and 5.6 from left to right, respectively.

The velocity errors from the CN method in Step 1 are larger, while the ones with BDF2 method in 1 are smaller, especially in the left plot of Figure 5.5, where the error curve for BDF2 is very close to the horizontal-axis, and thus hard to observe on the graph.

5.4. Rotating flow between offset cylinders. Finally we compare four options (CN with no Step 2, BDF2 with no Step 2, CN with Step 2 and BDF2 with Step 2) on a problem motivated by the classic problem of flow between rotating cylinders. We take the domain to be a disk with a smaller, off center, obstacle inside. Let $r_1 = 1, r_2 = 0.1, c = (c_1, c_2) = (\frac{1}{2}, 0)$,

$$\Omega = \{(x, y) : x^2 + y^2 \leq r_1^2 \text{ and } (x - c_1)^2 + (y - c_2)^2 \geq r_2^2\}.$$

The boundary conditions are no slip, $Re = 250$ and the flow is driven by a body force (rather than rotation of either cylinder)

$$f(x, y) = (-2y, 2x)$$

which induces a counter clockwise rotation. The flow rotates about $(0, 0)$, interacts with the immersed cylinder $(x - c_1)^2 + (y - c_2)^2 \leq r_2^2$ which induces a von Kármán vortex street. This vortex street rotates

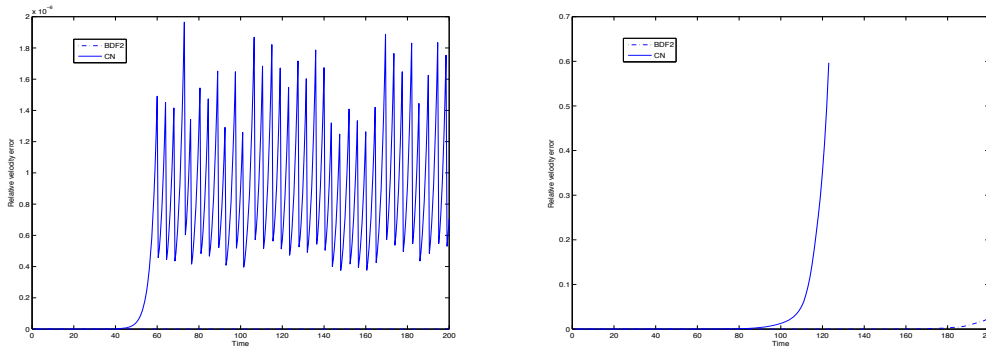


Fig. 5.5: The development of relative velocity error in time for $\Delta t = 0.5$, $\Delta t = 1$, from left to right: CN large, and BDF2 error came close to x -axis (very small).

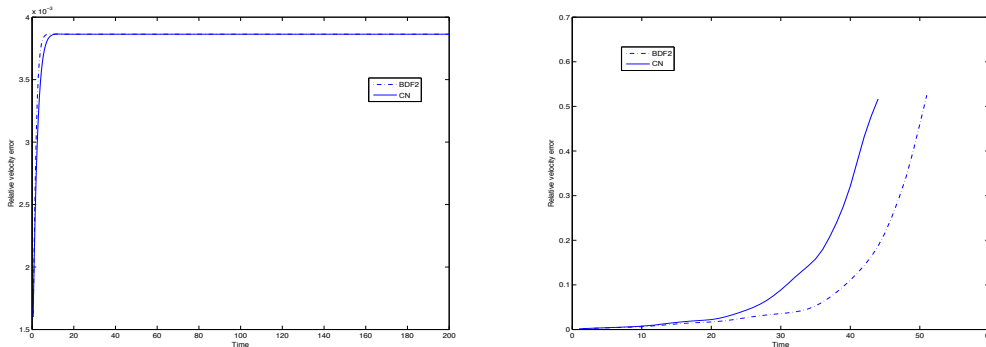


Fig. 5.6: The development of relative velocity error in time for $\Delta t = 0.5$, $\Delta t = 1$ with perturbed initial condition, from left to right.

and itself re-interacts with the immersed cylinder, creating more complex structures. This flow also contains complex structures in the boundary layer near $x^2 + y^2 = r_1^2$ which are not resolved on the mesh. (To resolve these would require a mesh with at least 3 points within $O(1/Re) = O(1/250)$ of each wall.) The mesh is parameterized by the number of mesh points around the outer cylinder ($n = 40$ and 60) and $\frac{n}{4}$ mesh points around the immersed cylinder, and extended to all of Ω as a Delaunay mesh. See Figure 5.7 for the coarsest $n = 20$ mesh. ¹

We give plots over $0 \leq t \leq 40$ of the following quantities:

$$A(t) := \|\mathbf{x} \cdot \mathbf{u}\| \doteq \text{angular momentum},$$

$$\|\text{curl } \mathbf{u}\| = \text{RMS vorticity}, \|\text{grad } \mathbf{u}\|^2 = \frac{1}{\nu} * \text{enstrophy}.$$

All four are inviscid invariants of $2d$ flows without boundaries. Three are interesting for rotational flows. We selected $\Delta t = 0.01$. Our observations on this interesting flow are preliminary, not intended to describe flow details and only intended to *test the effects of Step 2 on the global balance in four important quantities*.

¹An expanded version of this report is available at <http://www.mathematics.pitt.edu/research/technical-reports.php> containing plots of the $n = 20$ case and plots of energy vs. time for $n = 40$ and 60 .

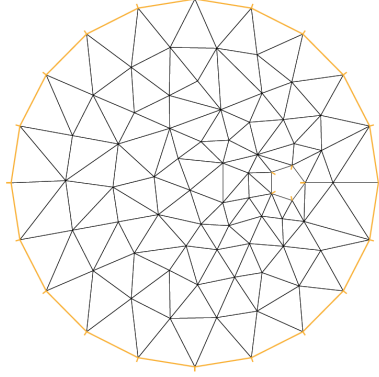


Fig. 5.7: The coarsest mesh using $n = 20$ points around immersed cylinder.

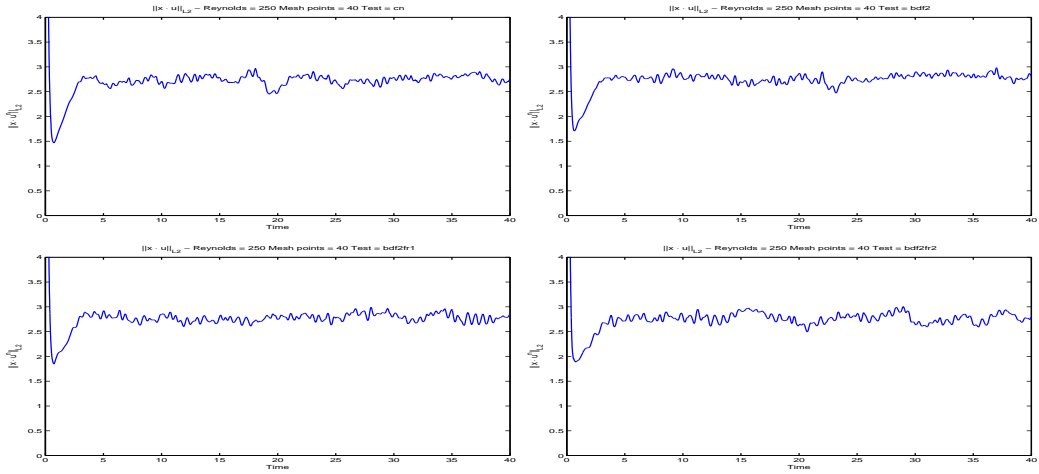


Fig. 5.8: Angular momentum $Re = 250$, $N = 40$ mesh points around outer cylinder.

For $N = 40$ points around outer cylinder, the increased resolution near the immersed cylinder allows more rotational structures. This results in a 50% increase in angular momentum over the $N = 20$ case (not given here). The plots of $\|\text{grad } \mathbf{u}\|^2$ also increased by 50% over the $N = 20$ case indicating that regularizations which dissipate energy are necessary to model the energy dissipated by unresolved structures.

The plots of $\|\text{curl } \mathbf{u}\|$ do not seem to be over-smoothed by the addition of Step 2. When $N = 60$ points around the outer cylinder, CN still show the effect of an initial transient in $A(t)$ (present in all previous angular momentum plots). This transient is nearly eliminated in the test of CN with Step 2 and BDF with Step 2.

For the CN method without Step 2 we also find the average value of enstrophy increases substantially when N increases from 40 to 60. No evidence of under-diffusion is seen in the plots of global enstrophy which include Step 2: the mean value of the enstrophy does not increase from $N = 40$ to $N = 60$.

6. Conclusions. The BDF2 time discretization is second order, A-stable and has stability properties that are superior to those of Crank-Nicolson for underresolved flow simulations. We have seen that modular stabilization by *filter, then stabilize* works well in combination with BDF2. The nu-

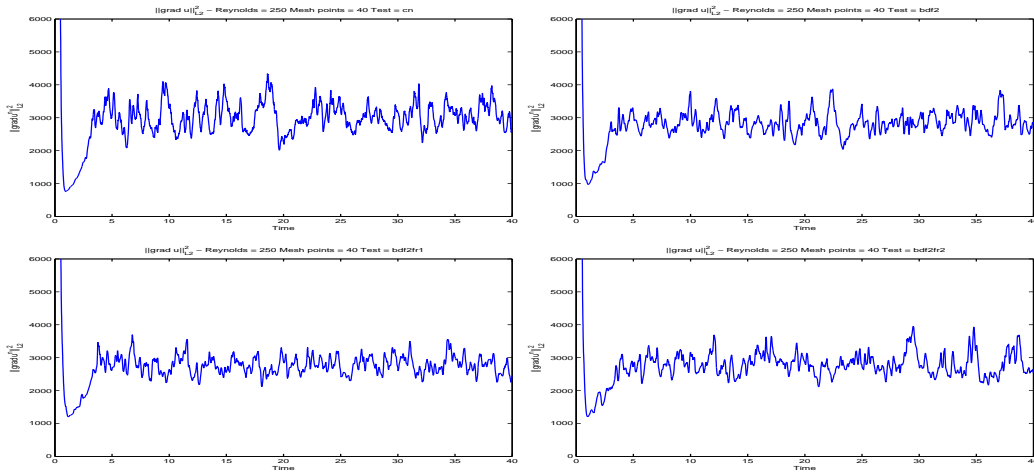


Fig. 5.9: $\|\text{grad } \mathbf{u}\|_2^2$, $\text{Re} = 250$, $N = 40$ mesh points around outer cylinder.

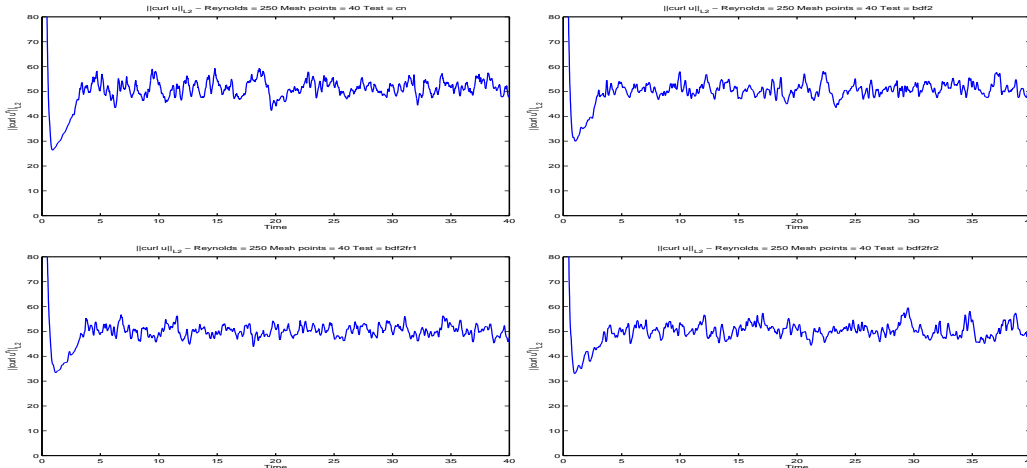


Fig. 5.10: Vorticity, $\text{Re} = 250$, $N = 40$ mesh points around outer cylinder.

numerical experiments confirm the stability and convergence theory and show that this combination much better than unstabilized methods and somewhat better than Crank-Nicolson plus is the same stabilization.

The correct scaling of the relaxation parameter χ seems to be $\chi = O(\Delta t)$. However, the precise determination of χ step by step so as to match numerical dissipation to that occurring on unresolved scales is an important open problem.

Acknowledgment. We thank Dr. Myron Sussman for his constructive comments and help with the numerical section of this paper. This research was partially supported by the NSF under grant DMS-0810385 (W. Layton, N. Mays) and by the Air Force under grant FA9550-09-1-0058 (C. Trechea).

REFERENCES

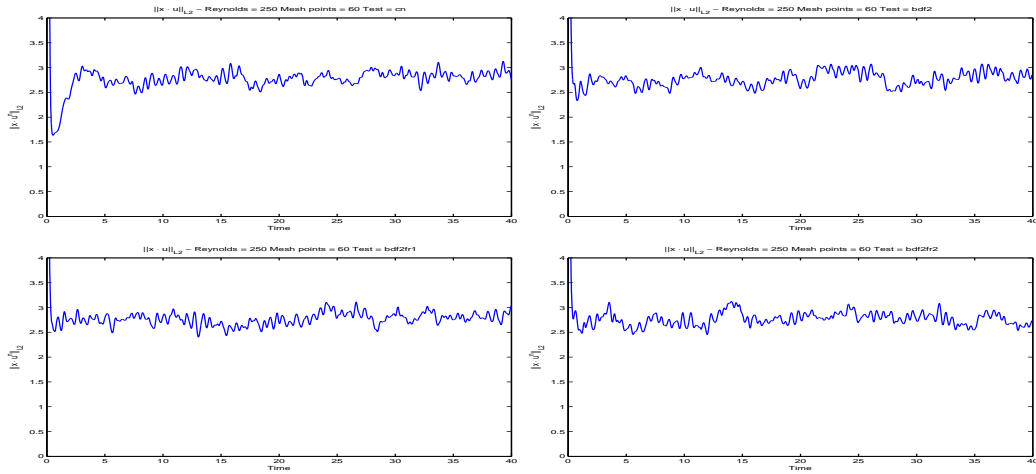


Fig. 5.11: Angular momentum, $Re = 250$, $N = 60$ mesh points around outer cylinder.

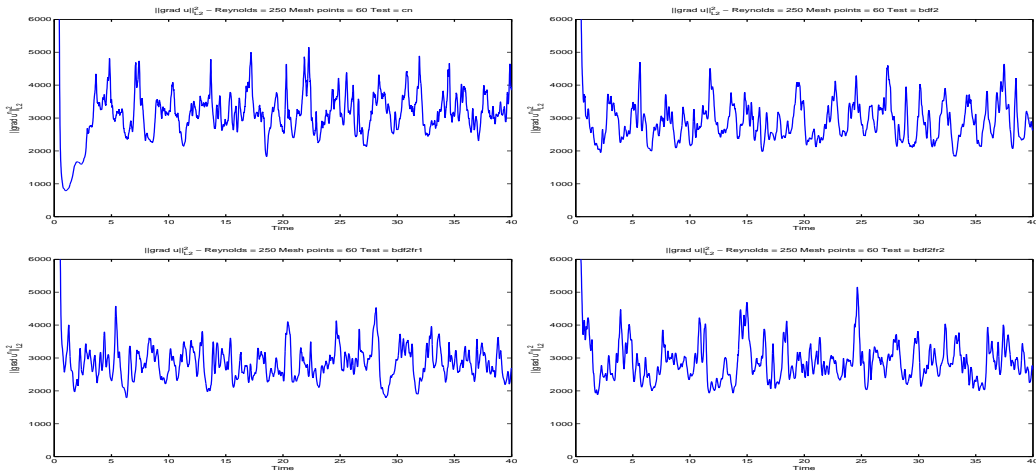


Fig. 5.12: $\|\text{grad } \mathbf{u}\|^2$, $Re = 250$, $N = 60$ mesh points around outer cylinder.

- [1] N. ADAMS AND A. LEONARD, *Deconvolution of subgrid scales for the simulation of shock-turbulence interaction*, in Direct and Large Eddys Simulation III, N. S. P. Voke and L. Kleiser, eds., Kluwer, Dordrecht, 1999, p. 201.
- [2] N. ADAMS AND S. STOLZ, *Deconvolution methods for subgrid-scale approximation in large-eddy simulation*, Modern Simulation Strategies for Turbulent Flow, R.T. Edwards, 2001.
- [3] ———, *A subgrid-scale deconvolution approach for shock capturing*, J. Comput. Phys., 178 (2002), pp. 391–426.
- [4] G. A. BAKER, V. A. DOUGALIS, AND O. A. KARAKASHIAN, *On a higher order accurate fully discrete Galerkin approximation to the Navier-Stokes equations*, Math. Comp., 39 (1982), pp. 339–375.
- [5] D. BARBATO, L. C. BERSELLI, AND C. R. GRISANTI, *Analytical and numerical results for the rational large eddy simulation model*, J. Math. Fluid Mech., 9 (2007), pp. 44–74.
- [6] L. BERSELLI, C. GRISANTI, AND V. JOHN, *On commutator errors in the divergence of the space averaged Navier-Stokes equations*.
- [7] L. C. BERSELLI, *On the large eddy simulation of the Taylor-Green vortex*, J. Math. Fluid Mech., 7 (2005), pp. S164–S191.
- [8] J. P. BOYD, *Two comments on filtering (artificial viscosity) for Chebyshev and Legendre spectral and spectral element methods: preserving boundary conditions and interpretation of the filter as a diffusion*, J. Comput.

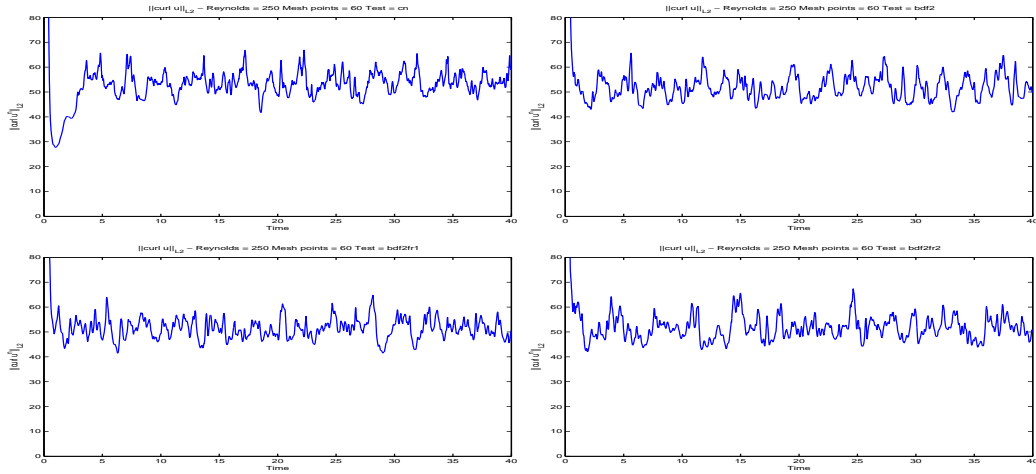


Fig. 5.13: Vorticity, $Re = 250$, $N = 60$ mesh points around outer cylinder.

- Phys., 143 (1998), pp. 283–288.
- [9] S. C. BRENNER AND L. R. SCOTT, *The mathematical theory of finite element methods*, vol. 15 of Texts in Applied Mathematics, Springer-Verlag, New York, 1994.
- [10] C. CANUTO, M. Y. HUSSAINI, A. QUARTERONI, AND T. A. ZANG, *Spectral methods*, Scientific Computation, Springer, Berlin, 2007. Evolution to complex geometries and applications to fluid dynamics.
- [11] A. CHORIN, *Numerical solution for the Navier-Stokes equations*, Math. Comp., 22 (1968), pp. 745–762.
- [12] J. CONNORS AND W. LAYTON, *On the accuracy of the finite element method plus time relaxation*, Math. Comp., 79 (2010), pp. 619–648.
- [13] A. DUNCA, *Investigation of a shape optimization algorithm for turbulent flows*, tech. rep., Argonne National Lab, report number ANL/MCS-P1101-1003, 2002, <http://www-fp.mcs.anl.gov/division/publications/>.
- [14] ———, *Space averaged Navier Stokes equations in the presence of walls*, PhD thesis, University of Pittsburgh, 2004.
- [15] A. DUNCA AND Y. EPSHTEYN, *On the Stolz-Adams deconvolution model for the large-eddy simulation of turbulent flows*, SIAM J. Math. Anal., 37 (2006), pp. 1890–1902 (electronic).
- [16] E. EMMRICH, *Error of the two-step BDF for the incompressible Navier-Stokes problem*, M2AN Math. Model. Numer. Anal., 38 (2004), pp. 757–764.
- [17] V. ERVIN, W. LAYTON, AND M. NEDA, *Numerical analysis of a higher order time relaxation model of fluids*, Int. J. Numer. Anal. Model., 4 (2007), pp. 648–670.
- [18] ———, *Numerical analysis of filter based stabilization for evolution equations*, tech. rep., University of Pittsburgh, 2010.
- [19] P. FISCHER AND J. MULLEN, *Filter-based stabilization of spectral element methods*, C. R. Acad. Sci. Paris Sér. I Math., 332 (2001), pp. 265–270.
- [20] E. GARNIER, N. ADAMS, AND P. SAGAUT, *Large eddy simulation for compressible flows*, Scientific Computation, Springer, Berlin, 2009.
- [21] V. GIRAULT AND P.-A. RAVIART, *Finite element approximation of the Navier-Stokes equations*, vol. 749 of Lecture Notes in Mathematics, Springer-Verlag, Berlin, 1979.
- [22] M. D. GUNZBURGER, *Finite element methods for viscous incompressible flows*, Computer Science and Scientific Computing, Academic Press Inc., Boston, MA, 1989. A guide to theory, practice, and algorithms.
- [23] F. HECHT AND O. PIRONNEAU, *Freefem++*, webpage: <http://www.freefem.org>.
- [24] J. G. HEYWOOD AND R. RANACHER, *Finite-element approximation of the nonstationary Navier-Stokes problem. IV. Error analysis for second-order time discretization*, SIAM J. Numer. Anal., 27 (1990), pp. 353–384.
- [25] V. JOHN, *Large eddy simulation of turbulent incompressible flows*, vol. 34 of Lecture Notes in Computational Science and Engineering, Springer-Verlag, Berlin, 2004. Analytical and numerical results for a class of LES models.
- [26] V. JOHN AND W. J. LAYTON, *Analysis of numerical errors in large eddy simulation*, SIAM J. Numer. Anal., 40 (2002), pp. 995–1020.
- [27] W. LAYTON, *Superconvergence of finite element discretization of time relaxation models of advection*, BIT, 47 (2007), pp. 565–576.

- [28] W. LAYTON, *A remark on regularity of an elliptic-elliptic singular perturbation problem*, tech. rep., University of Pittsburgh, <http://www.mathematics.pitt.edu/research/technical-reports.php>, 2007.
- [29] W. LAYTON, C. MANICA, M. NEDA, AND L. REBHOLZ, *Helicity and energy conservation and dissipation in approximate deconvolution LES models of turbulence*, *Adv. Appl. Fluid Mech.*, 4 (2008), pp. 1–46.
- [30] W. LAYTON AND M. NEDA, *Truncation of scales by time relaxation*, *J. Math. Anal. Appl.*, 325 (2007), pp. 788–807.
- [31] W. LAYTON, L. G. REBHOLZ, AND C. TRENCHEA, *Modular nonlinear filter stabilization of methods for higher Reynolds numbers flow*, *J. Math. Fluid Mech.*, to appear (2011).
- [32] W. LAYTON, L. RÖHE, AND H. TRAN, *Explicitly uncoupled VMS stabilization of fluid flow*, tech. rep., University of Pittsburgh, 2010.
- [33] J. MATHEW, R. LECHNER, H. FOYSI, J. SESTERHENN, AND R. FRIEDRICH, *An explicit filtering method for large eddy simulation of compressible flows.*, *Phys. Fluids*, 15 (2003).
- [34] J. S. MULLEN AND P. F. FISCHER, *Filtering techniques for complex geometry fluid flows*, *Comm. Numer. Methods Engrg.*, 15 (1999), pp. 9–18.
- [35] S. RAVINDRAN, *Convergence of extrapolated BDF2 finite element schemes for unsteady penetrative convection model*, *Numerical Functional Analysis and Optimization*, (2011).
- [36] P. ROSENAU, *Extending hydrodynamics via the regularization of the Chapman-Enskog expansion*, *Phys. Rev.A*, 40 (1989), p. 7193.
- [37] M. SCHÄFER AND S. TUREK, *Benchmark computations of laminar flow around cylinder*, in *Flow Simulation with High-Performance Computers II*, H. EH, ed., vol. 52, Vieweg, 1996, pp. 547–566.
- [38] S. SCHOCHET AND E. TADMOR, *The regularized Chapman-Enskog expansion for scalar conservation laws*, *Arch. Rat. Mech. Anal.*, 119 (1992), p. 95.
- [39] I. STANCULESCU, *Existence theory of abstract approximate deconvolution models of turbulence*, *Ann. Univ. Ferrara Sez. VII Sci. Mat.*, 54 (2008), pp. 145–168.
- [40] S. STOLZ AND N. ADAMS, *On the approximate deconvolution procedure for LES*, *Phys. Fluids*, II (1999), pp. 1699–1701.
- [41] S. STOLZ, N. ADAMS, AND L. KLEISER, *An approximate deconvolution model for large eddy simulation with application to wall-bounded flows*, *Phys. Fluids*, 13 (2001), pp. 997–1015.
- [42] ———, *The approximate deconvolution model for LES of compressible flows and its application to shock-turbulent-boundary-layer interaction*, *Phys. Fluids*, 13 (2001), p. 2985.
- [43] ———, *The approximate deconvolution model for compressible flows: isotropic turbulence and shock-boundary-layer interaction*, in *Advances in LES of Complex Flows*, R. Friedrich and W. Rodi, eds., vol. 65 of *Fluid Mechanics and Its Applications*, Springer, Netherlands, 2002, pp. 33–47.
- [44] D. TAFTI, *Comparison of some upwind-biased high-order formulations with a second-order central-difference scheme for time integration of the incompressible Navier-Stokes equations*, *Comput. & Fluids*, 25 (1996), pp. 647–665.
- [45] G. TAYLOR, *On decay of vortices in a viscous fluid*, *Phil. Mag.*, 46 (1923), pp. 671–674.
- [46] G. I. TAYLOR AND A. E. GREEN, *Mechanism of the production of small eddies from large ones*, *Proceedings of the Royal Society of London. Series A*, 158 (1937), pp. pp. 499–521.
- [47] M. VISBAL AND D. RIZZETTA, *Large-eddy simulation on general geometries using compact differencing and filtering schemes*, *AIAA Paper*, 2002-288.
- [48] X. WANG, *A second order in time scheme for approximating long time statistical properties of the two dimensional Navier-Stokes equations*, preprint, (2011).
- [49] E. ZEIDLER, *Applied functional analysis*, vol. 108 of *Applied Mathematical Sciences*, Springer-Verlag, New York, 1995.